Effects of River Channel Structural Modifications on High-Flow Characteristics Using 2D Rain-on-Grid HEC-RAS Modelling: A Case of Chongwe River Catchment in Zambia

Frank Mudenda *, Hosea Mwangi, John M. Gathenya, Caroline W. Maina

Posted Date: 31 December 2025

doi: 10.20944/preprints202512.2831.v1

Keywords: Chongwe Catchment; HEC-RAS; 2D rain-on-grid modelling; high flows; concrete-lining; stormwater drainage systems; structural modifications

 doi:10.20944/preprints202512.2831.v1

Article

Effects of River Channel Structural Modifications on High-Flow Characteristics Using 2D Rain-on-Grid HEC-RAS Modelling: A Case of Chongwe River Catchment in Zambia

Frank Mudenda [1,2,*], Hosea Mwangi [1], John M. Gathenya [1] and Caroline W. Maina [3]

[1] Department of Soil, Water and Environmental Engineering, Jomo Kenyatta University of Agriculture and Technology, P.O. Box 62000 – 00200, Nairobi, Kenya

[2] Department of Civil and Environmental Engineering, University of Zambia, PO Box 32379, Lusaka, Zambia

[3] Department of Agricultural Engineering, Egerton University, P.O. Box 536 – 20115, Egerton-Njoro, Kenya

* Correspondence: frank.mudenda@students.jkuat.ac.ke or frank_mudenda@yahoo.com

Abstract

With accelerating climate change and urbanization, river catchments continue to experience structural modifications through dam construction and concrete-lining of natural channels as adaptation measures. These interventions can alter the natural hydrology. This necessitates assessment of their influence on hydrology at a catchment scale. However, such evaluations are particularly challenging in data-scarce regions such as the Chongwe River Catchment, where hydrometric records capturing conditions before and after structural modifications are limited. Therefore, we applied a 2D rain-on-grid approach in HEC-RAS to evaluate changes in high-flow characteristics in the Chongwe River Catchment in Zambia, where structural interventions have been implemented. The terrain was modified in HEC-RAS to represent 21 km of concrete drains and ten dams. Sensitivity analysis was conducted on five model parameters and showed that Manning's roughness coefficient had by far the largest impact on peak flows. Model calibration and validation showed strong performance with R^2 = 0.99, NSE = 0.75 and PBIAS = – 0.68 % during calibration and R^2 = 0.95, NSE = 0.75, PBIAS = – 2.49 % during validation. Four scenarios were simulated to determine the hydrological effects of channel concrete-lining and dams. The results showed that concrete-lining of natural channels in the urban area increased high flows at the main outlet by approximately 4.6%, generated very high channel velocities of up to 20 m/s, increased flood depths by up to 11%, and expanded flood extents by up to 15%. The existing dams reduced peak flows by about 28%, increased lag times, reduced flood depths by about 11%, and reduced flood extents by up to 8% across the catchment. The findings demonstrate that enhancing stormwater conveyance through concrete-lining must be complemented by storage to manage high flows, while future work should explore nature-based solutions to reduce channel velocities and improve sustainable flood mitigation.

Keywords: Chongwe Catchment; HEC-RAS; 2D rain-on-grid modelling; high flows; concrete-lining; stormwater drainage systems; structural modifications

1. Introduction

Climate change remains one of the most formidable global challenges of the twenty-first century, exerting profound impacts on hydrological systems, ecosystems, and human livelihoods [1]. Increasing evidence shows that intensifying climatic change has led to more frequent and severe floods, droughts, and prolonged dry spells, disrupting agricultural productivity and threatening water and food security worldwide [1–3]. Globally, such events have displaced an estimated 22 million people annually since 2008, emphasizing the growing humanitarian extent of hydrological

 doi:10.20944/preprints202512.2831.v1

extremes [4]. Global assessments further indicate that under continued warming, some regions will experience enhanced surface runoff and flood risk, while others will face pronounced drying trends [3]. The Intergovernmental Panel on Climate Change (IPCC) Sixth Assessment Report projects a potential rise in global mean temperature of up to 1.5 °C above pre-industrial levels by the early 2030s, accompanied by intensified precipitation extremes, prolonged droughts, and accelerated sea-level rise between 0.3 m and 1.1 m by 2100 [1]. These shifts are continually driving countries around the world to adopt adaptation measures to enhance resilience and mitigate escalating hydrological risks at both local and basin scales [5–7].

In response to these evolving climatic pressures, structural interventions have become central to national and regional adaptation strategies across many parts of the world. Governments and water management authorities are increasingly constructing dams, retention basins, and concrete-lined drainage systems to control floods and secure water supply for domestic and agricultural use [8]. While such measures play a vital role in safeguarding infrastructure and livelihoods, they also introduce significant alterations to natural hydrological regimes [5]. These modifications change infiltration capacity, channel roughness, and storage dynamics, thereby influencing the magnitude, timing, and duration of peak flows [9]. Previous studies have reported that channel concretization accelerates runoff concentration and reduces groundwater recharge, whereas dam construction alters downstream hydrographs [7,10,11]. Understanding the impact of these measures on runoff in a watershed is a critical aspect of water resource management and hydrological studies [12–14]. For instance, Huang et al. [15] demonstrated that increased structural modification by increasing imperviousness hindered the infiltration of runoff and caused it to flow directly into rivers, ultimately increasing both surface and channel runoff. Their findings gave implications for prioritizing measures in flood prevention and preparedness, such as the consideration of building arrangement, green infrastructure, and the Low Impact Development (LID) techniques.

Assessing the effects of interventions has become an essential component of modern watershed management and climate adaptation planning [16,17]. Researchers have employed approaches to evaluate the hydrological impacts of anthropogenic interventions in watershed systems. Studies such as those by Rose and Peters [18], Miller et al. [19] and Ress et al. [6] applied paired-catchment analyses to compare runoff responses between drained and undrained basins, demonstrating that artificial drainage increases surface runoff and shortens flow concentration times. More recent studies have advanced to process-based and data-driven frameworks that couple hydrological and statistical methods [20–22]. For instance, Song et al. [20] combined the SIMHYD rainfall–runoff model, the Budyko framework, and double-mass curve (DMC) analysis to quantify the hydrological alterations induced by mining in the headwaters of Chinese catchments, reporting consistent evidence of substantial flow modification across all methods. Similarly, Zhang et al. [21] used both DMC and hydrological modelling to assess irrigation and mining impacts in the Qingshui River Basin, revealing significant declines in streamflow. While the DMC technique provides a simple means of detecting regime shifts, it cannot reproduce natural flow processes under non-stationary or structurally modified conditions, or during specific rainfall events [23]. In contrast, physically based hydrological models have demonstrated greater capability to reproduce natural streamflow regimes because they incorporate watershed characteristics such as soils, slopes, land use, and climatic variables [20,24]. When integrated with hydraulic analysis, these models can effectively capture spatially distributed hydrological responses to observed rainfall events by accounting for both channel and catchment-scale flow dynamics [25].

HEC-RAS two-dimensional (2D) rain-on-grid modelling has emerged as a powerful approach for simulating coupled hydrologic–hydraulic processes. Its rain-on-grid capability enables direct application of rainfall events onto a two-dimensional computational mesh, allowing dynamic interaction between surface runoff, catchment characteristics, and channel flow [26]. Despite its growing use in floodplain and urban drainage studies worldwide [8,11,27], few studies have employed this approach to evaluate the effects of structural interventions such as dam storage and concrete-lined drains on high-flow behaviour at a catchment scale. In addition, the simulation

 doi:10.20944/preprints202512.2831.v1

structural interventions form a scientific basis for identifying locations where Nature-Based Solutions (NbS) can be implemented and would most effectively enhance flood mitigation and complement existing civil engineering infrastructure [16,28,29].

This study seeks to contribute knowledge by assessing the high-flow characteristics of the Chongwe River Catchment in Zambia using HEC-RAS 6.5, particularly terrain modification tools. Terrain modification provides a low-cost approach for adjusting freely available DEMs to incorporate small-scale engineered features without the need for detailed topographic surveys, such as drone-based mapping [30]. Within the Chongwe Catchment, two major structural-based interventions have already been implemented, namely: (i) concrete-lining of natural river channels in urban Lusaka for flood management, and (ii) construction of ten dams on the rivers primarily for irrigation and domestic water supply [31–33]. Despite their scale and significance, the hydrological impacts of these measures on the observed high-flow characteristics of the Chongwe River during extreme rainfall events remain poorly understood at the catchment scale. Moreover, to the best of our knowledge, no study has undertaken rainfall-event-based modelling of flows within the Chongwe Catchment. Our study, therefore, provides a low-cost novel approach to how engineered river catchment modifications affect hydrological responses, giving transferable approaches for assessing infrastructure-driven flood dynamics in data-scarce river catchments and an opportunity for improvement in future planning.

2. Materials and Methods

2.1. Study Area

This study was conducted in the Chongwe River Catchment, located in south-central Zambia between latitudes 14.9°S and 15.5°S and the Longitudes of 28.2°E and 28.8°S (Figure 1). The catchment covers an area of approximately 1,964 km² and encompasses parts of the towns of Lusaka, Chongwe, and Chisamba. The mean annual rainfall ranges from 750 mm to 930 mm [34]. As shown in Figure 2, rainfall peaks in January with an average value of 232 mm. Minimum and maximum air temperatures are approximately 8.2 °C and 32 °C, respectively [32]. The mean annual actual evapotranspiration is about 786 mm [35] which peaks in March with a mean of 99 mm (Figure 2). Topographically, the catchment is relatively flat, with elevations varying between 1,041 m and 1,421 m above mean sea level. According to the Food and Agriculture Organization (FAO) soil classification, the dominant soil types in the catchment are Luvisols and Acrisols [34]. Considering vegetation, the Miombo woodland is predominant, characterized by semi-evergreen trees with a well-developed grass layer [35]. The Zambezi Escarpment zone, located in the catchment, is predominantly Mopane woodland, typically interspersed by patches of Munga woodland [36].

 doi:10.20944/preprints202512.2831.v1

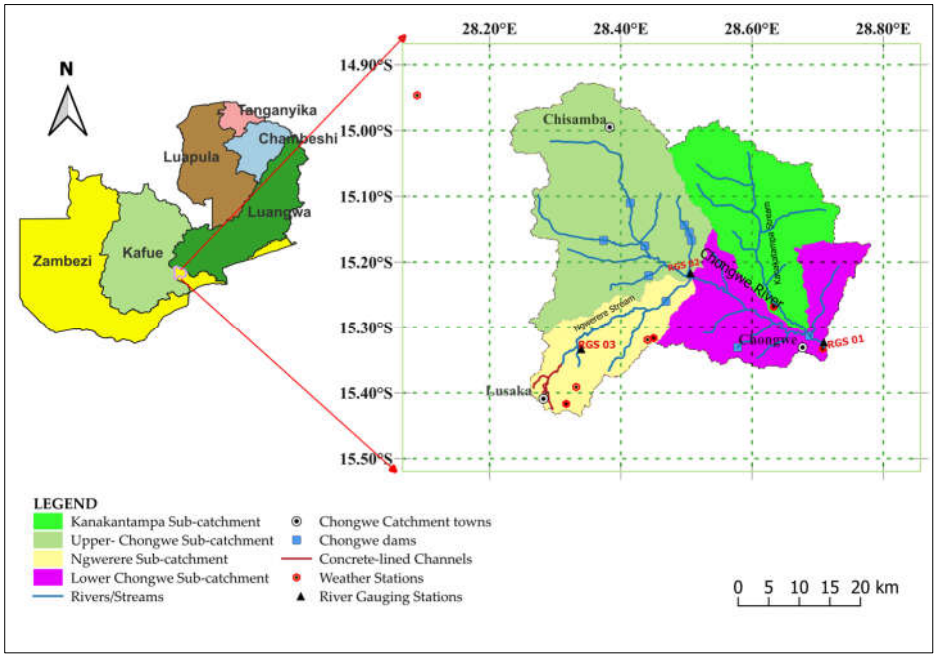

Figure 1. Location of the Chongwe River Catchment in Zambia showing sub-catchments, drainage features including rivers, concrete-lined channels and dams, as well as the locations of weather stations, river gauging stations and major towns.

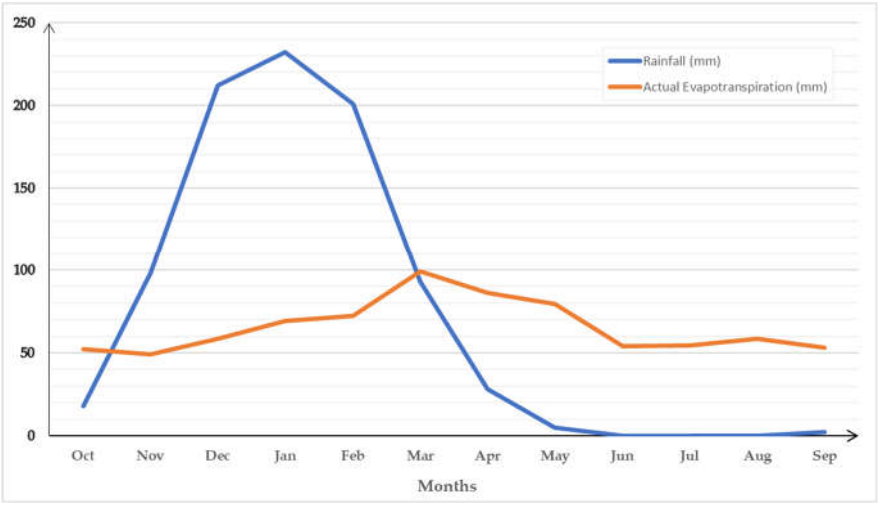

Figure 2. Averaged monthly rainfall (mm) and actual evapotranspiration (mm) of Chongwe Catchment.

The study area comprises four main sub-catchments (See Figure 1): Ngwerere, Upper Chongwe, Kanakantapa, and Lower Chongwe. Each sub-catchment has distinct land-use and hydrological characteristics influencing surface runoff generation and flood behaviour. The Ngwerere Sub-catchment, originating in urban Lusaka, represents the city's drainage outflow, where approximately 21 km of natural headwater channels have been concrete-lined to enhance flood conveyance from the city [31,37]. The Upper Chongwe Sub-catchment is dominated by commercial agriculture and contains the majority of irrigation infrastructure, hosting seven irrigation dams that support surface-water abstractions for crop production [38]. The Kanakantapa Sub-catchment reflects intensive rain-fed agriculture and livestock keeping associated with government farming blocks dominated by maize cultivation [39]. The Lower Chongwe Sub-catchment integrates flows from the urbanizing Chongwe Town and surrounding agricultural lands, containing two additional irrigation dams, while one small dam is located in the Ngwerere Sub-catchment. The outlet of the Lower Chongwe

 doi:10.20944/preprints202512.2831.v1

Sub-catchment, referred to as the Main Chongwe Outlet, serves as the principal monitoring point for evaluating cumulative catchment-scale hydrological responses. The summary of the characteristics of the sub-catchments is given in Table 1.

Table 1. Sub-catchments of the Chongwe River Catchment.

Sub-Catchment	Size (km²)	Predominant Land Use
Upper-Chongwe	809	Agriculture, Ranch, Irrigation
Ngwerere	289	Built up, Agriculture, Irrigation
Kanakantapa	482	Forest, Rainfed Agriculture, Settlements
Lower-Chongwe	384	Built-up, Agriculture
Total	1,964	

2.2. Methodological Approach

The modelling approach adopted in this study was implemented within HEC-RAS v6.5 using its RAS Mapper environment, which integrates spatial data for terrain generation, geometric configuration, and visualization of model outputs. The process involved developing a new terrain model from a Digital Elevation Model (DEM), refining it through terrain modification to represent concrete-lined channels and dam structures, and preparing input layers for rainfall, land use, and soils. The overall methodology applied in this study is summarized in Figure 3, which presents the sequential steps followed from data acquisition and pre-processing to model setup, calibration, validation, and scenario simulations. The outputs from the model runs include the flow, velocity, flood depths and flood extents. These were compared to determine the impacts of the catchment structural modifications on the high flows of the Chongwe Catchment.

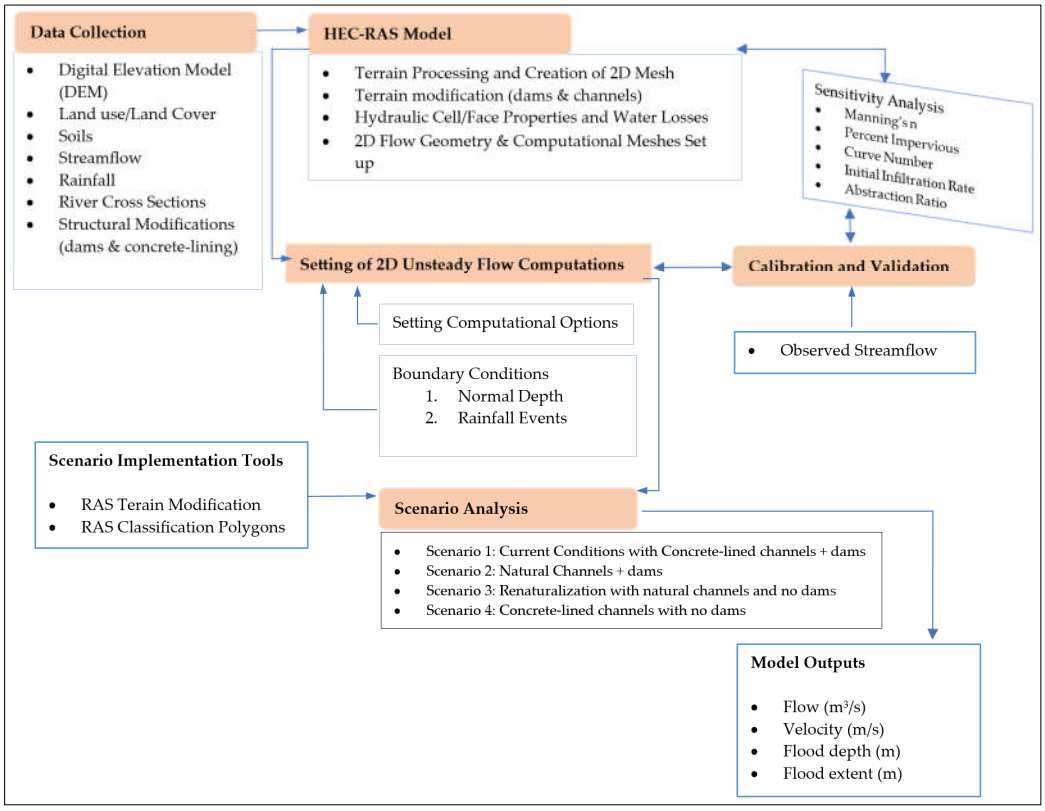

Figure 3. Overall Methodological Approach of the study.

 doi:10.20944/preprints202512.2831.v1

2.3. Data Collection and Sources

HEC-RAS 2D Rain-on-grid modelling involves incorporating geometric data to represent the hydrology and hydraulics of a river catchment. The datasets used in this study were acquired from multiple sources. The catchment boundary and river network were generated using the global watersheds tool [40]. The DEM (Figure 4) with 30 m resolution was obtained from the Japan Aerospace Exploration Agency (JAXA) [41]. The DEM provided essential topographic information for terrain processing and hydraulic geometry definition within HEC-RAS. To supplement the DEM in representing channels and dams, sample cross-sections at 16 locations (Figure 4) were collected from the Water Resources Management Authority (WARMA) and from field surveys using levelling and an Acoustic Doppler Current Profiler (ADCP v2.6) and used to modify terrain. Data on concrete-lined drainage channels, including layout and geometry (Figure 5), were obtained from the Lusaka City Council (LCC), and data on dams, including location and capacity, also shown in Figure 5, were sourced from the Department of Water Resources Development (DWRD), WARMA and Google Earth Pro. Ground-truthing surveys were conducted between December 2024 and June 2025 to verify channel geometry and dam locations.

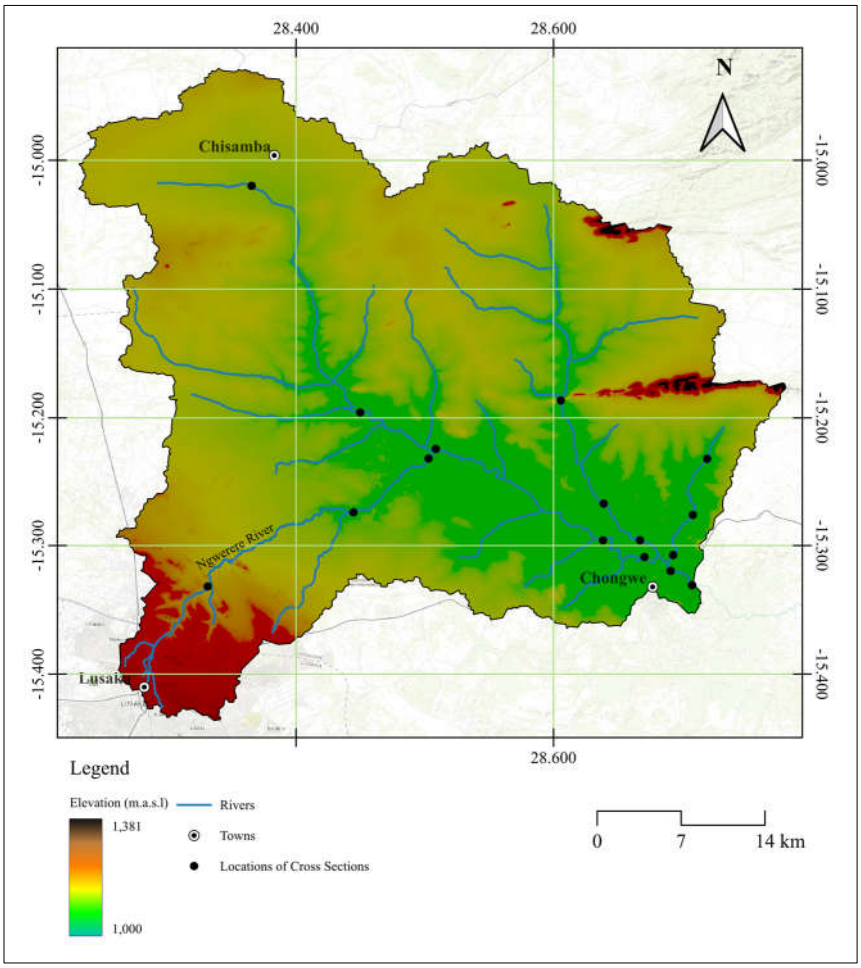

Figure 4. Digital Elevation Model and Location of Cross Sections.

 doi:10.20944/preprints202512.2831.v1

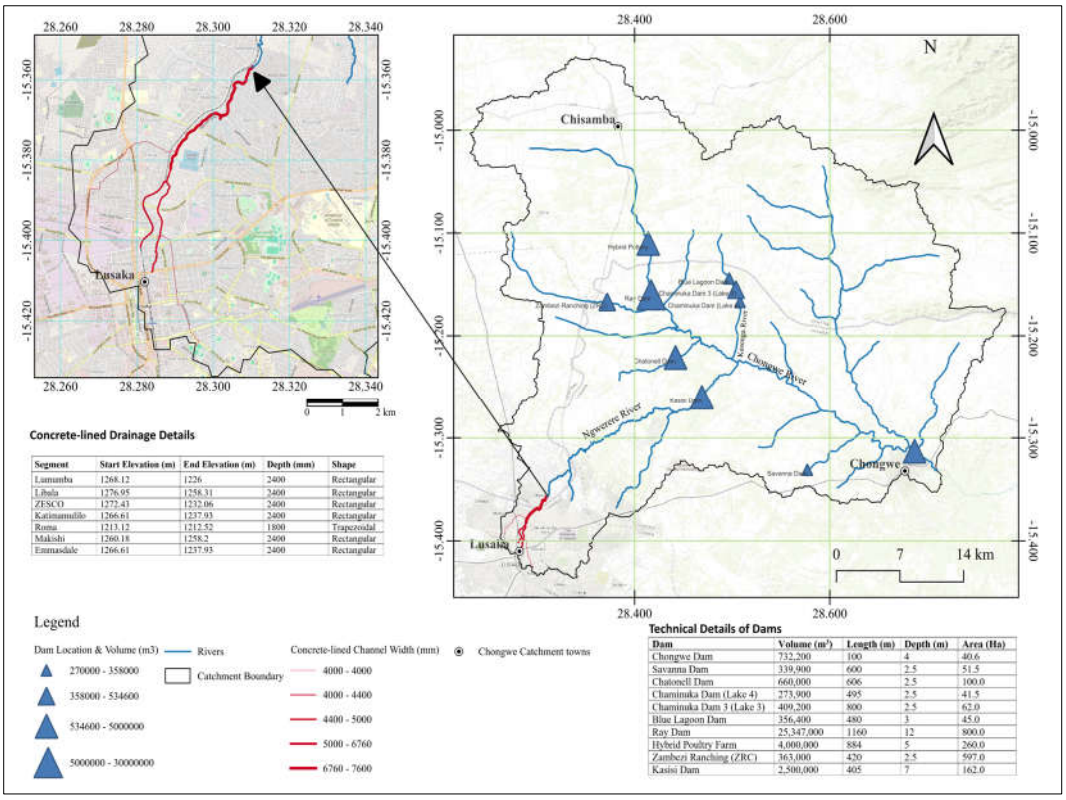

Figure 5. Location and details of the concrete-lined channel and existing dams.

To assign hydraulic properties to the computational cells in HEC-RAS, land-use/land-cover (LULC) and soil datasets are required. LULC (Figure 6a) was derived from the European Space Agency (ESA) WorldCover 2021 product with 10 m resolution accessed via Earth Map, based on Sentinel-1 and Sentinel-2 imagery while the soil dataset was obtained from the Hydrologic Soil Groups (HYSOGs250 m) database which provides a globally consistent gridded dataset of hydrologic soil groups (HSGs) with a geographic resolution of about 250 m [42]. Classification of HSGs (Figure 6b) was derived from soil-texture classes and depth-to-bedrock information provided by the FAO SoilGrids system [42]. The classification of the HSGs is described in Table 2. In addition, sub-hourly rainfall events at 15-minute intervals were collected from the SASSCAL Weathernet [41] at the Kenneth Kaunda International Airport and City Airport for the period October 2013 to February 2025 and used in the setting boundary conditions. Streamflow events at 15-minute intervals were collected from the WARMA for the Great East Road Bridge Gauging Station (RG1 shown in Figure 1) and used for model calibration and validation.

Table 2. Description of Hydrologic Soil Groups [42].

HSG	Description
A	Low runoff potential (>90% sand and <10% clay)
B	Moderately low runoff potential (50–90% sand and 10–20% clay)
C	Moderately high runoff potential (<50% sand and 20–40% clay)
D	High runoff potential (<50% sand and >40% clay)
A/D	High runoff potential unless drained (>90% sand and <10% clay)
B/D	High runoff potential unless drained (50–90% sand and 10–20% clay)
C/D	High runoff potential unless drained (<50% sand and 20–40% clay)
D/D	High runoff potential unless drained (<50% sand and >40% clay)

 doi:10.20944/preprints202512.2831.v1

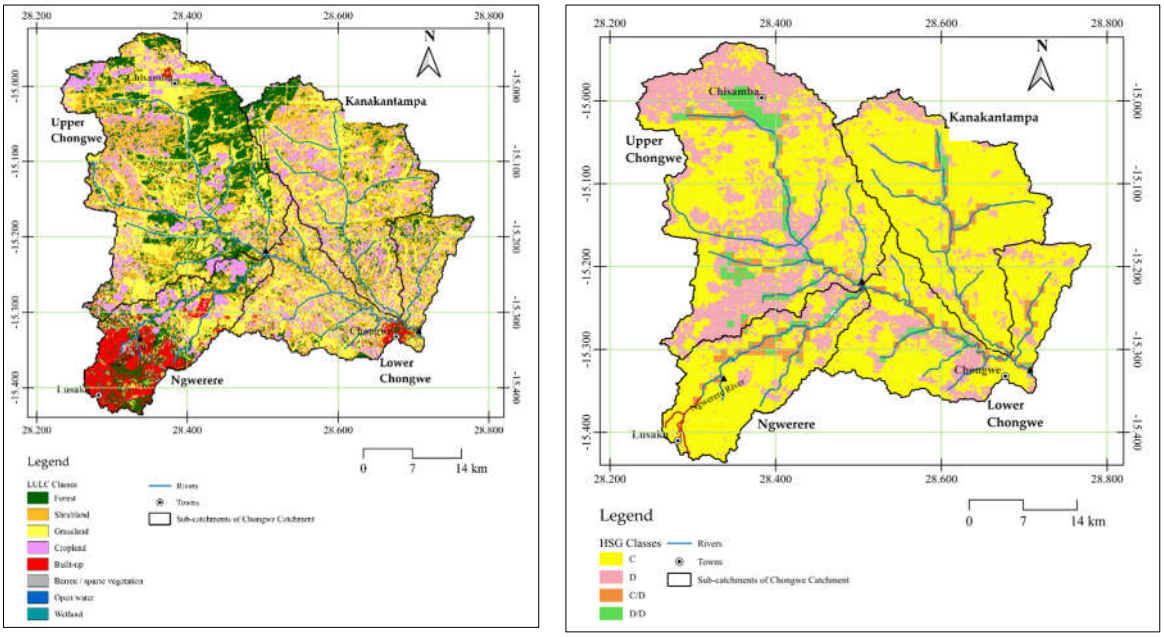

Figure 6. (**a**) LULC map of the Catchment; (**b**) Hydrological Soil Groups (HSGs) of the Catchment.

2.4. HEC-RAS Model Development

2.4.1. Terrain Processing

The terrain model forms the foundation for representing surface topography and flow pathways within the HEC-RAS 2D environment [43]. The 30 m DEM was pre-processed in Quantum Geographic Information System (QGIS) to ensure hydrological correctness and representation. However, the raw DEM did not represent the terrain below the water surface in the rivers and drainage channel geometry due to the DEM's coarse resolution. To improve this representation, 16 river cross-sections (Table S1 in supplementary data) from field surveys, Google Earth Pro and WARMA were integrated through terrain modification in RAS Mapper using a one-dimensional (1D) geometry. Since the cross-sections were few, the interpolation option [30] was used in HEC-RAS to estimate channel geometry between the available cross-section locations. The terrain modification channel and high ground tools in HEC-RAS were further applied to incorporate the geometry of concrete-lined drainage channels and dam walls, respectively, for better representation of channels and dam walls as recommended in the manual [30]. Figures 7 and S1 in the supplementary section show part of the original terrain model and the modified terrain model.

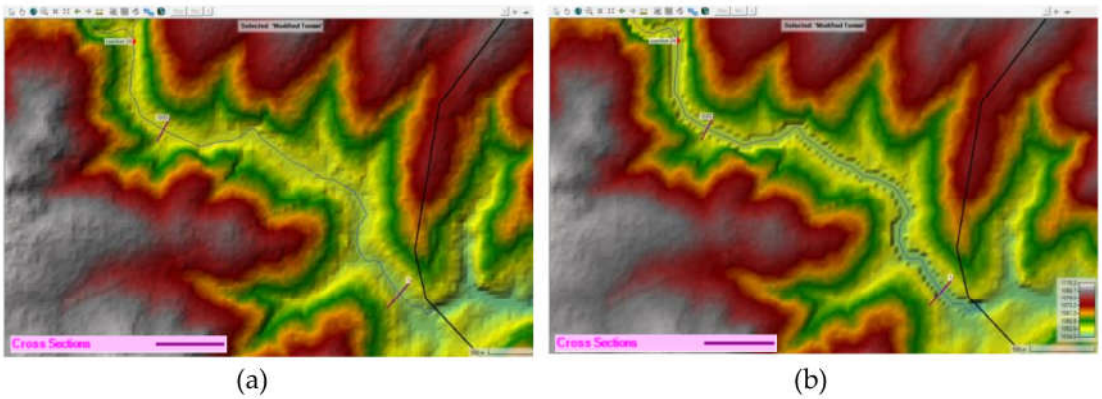

Figure 7. (a) Original terrain model; (b) Modified terrain model.

 doi:10.20944/preprints202512.2831.v1

2.4.2 Two-dimensional (2D) Flow Geometry and Computational Mesh Setup

A 2D flow area (Figure 8) was developed to mimic the hydrological response of the Chongwe River Catchment during rainfall events. A well-developed mesh is essential for numerical stability and for accurately simulating inundation patterns and high-flow routing [44]. A general grid resolution of 100 m was applied to the wider floodplain areas to balance accuracy, stability, computational efficiency and run-time [45]. Breaklines were used to introduce higher-resolution meshes around the rivers, drainage channels, bridges, and highlands to improve the representation of sharp hydraulic gradients and local flow dynamics. The 2D flow area was updated, having 406,706 computational cells generated and formed the basis of the simulations. Figure S2 in the supplementary materials shows the summarized characteristics of the 2D flow area.

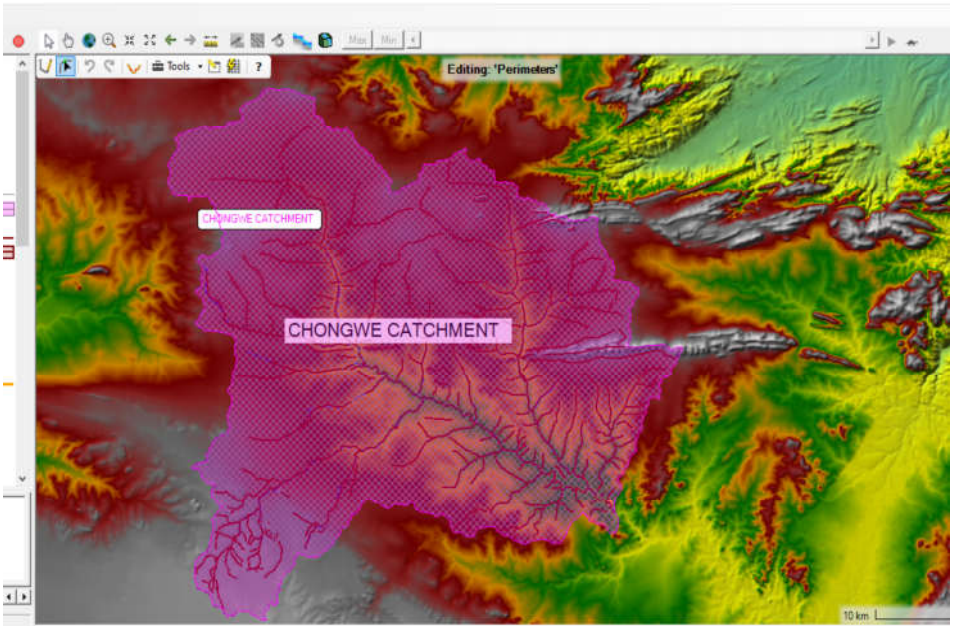

Figure 8. Developed computational mesh for 2D Flow Area (Red lines indicate breaklines; Background is the terrain model).

2.4.3 Hydraulic Cell/Face Properties and Water Losses

The hydraulic roughness and infiltration characteristics of the computational cells were defined to represent surface resistance and water losses during rainfall events. In HEC-RAS 2D, the hydraulic roughness of each cell was represented using Manning's n, assigned from the LULC layer and supported by literature recommendations [46]. The proportion of impervious area within each land-use class was also specified to account for areas where direct runoff dominates [47]. Classification polygons available under the LULC layer were used to assign Manning's n values to the concrete-lined drainage channels.

Water losses in HEC-RAS are computed using three available infiltration computation options: The Constant Deficit method, the SCS Curve Number method, and the Green-Ampt equation. Of these, the SCS Curve Number method was selected because it is widely applied in large-scale catchment studies, requires fewer site-specific soil hydraulic parameters compared to Green-Ampt, and provides a robust linkage between land use, soil type, and hydrologic response [48]. The input parameters for this method are the abstraction ratio, curve number and minimum infiltration (Table S2 in supplementary materials). These were assigned to the infiltration layer created by integrating the land use and soil characteristics as recommended by USDA SCS [30,47].

 doi:10.20944/preprints202512.2831.v1

2.4.4. Setting of 2D Unsteady Flow Computations

i) Computational Equations

HEC-RAS uses unsteady flow analyses to perform 2D simulations [43]. Unsteady 2D flood modelling advances in time the depth-averaged shallow-water Saint Venant's equations for a free surface over complex topography while exchanging water with rainfall, losses, and boundary fluxes under specified boundary conditions [30]. The governing equations used are as follows:

a. Continuity equation

$$\frac{\partial h}{\partial t} + \frac{\partial (hu)}{\partial x} + \frac{\partial (hv)}{\partial y} = \mathrm{r} - \mathrm{i} \qquad (1)$$

Where h = water depth (m), u, v = depth-averaged velocity components in x and y directions (m/s), t = time (s), r = rainfall intensity applied (m/s) and i = infiltration rate into the ground (m/s).

b. Momentum (x and y) equations

$$\frac{\partial (hu)}{\partial t} + \frac{\partial}{\partial x}(hu^2 + 0.5gh^2) + \frac{\partial (huv)}{\partial y} = -\mathrm{g}\, h\, S_{fx} \qquad (2)$$

$$\frac{\partial (hv)}{\partial t} + \frac{\partial (huv)}{\partial x} + \frac{\partial}{\partial y}(hv^2 + 0.5gh^2) = -\mathrm{g}\, h\, S_{fy} \qquad (3)$$

Where, g = gravitational acceleration [9.81 m/s²] and S_{fx}, S_{fy} = friction slope components in x and y directions (dimensionless)

c. Manning friction slopes

$$S_{fx} = \frac{n^2 u\sqrt{u^2+v^2}}{h^{4/3}}, \qquad (4)$$

$$S_{fy} = \frac{n^2 v\sqrt{u^2+v^2}}{h^{4/3}} \qquad (5)$$

Where n = Manning's roughness coefficient

In this study, the Diffusion Wave option was adopted as the computational shallow-water equation (SWE) solvers to implement equations (1-5) in HEC-RAS because it is well-suited to broad, mildly sloped floodplains and rainfall-driven sheet flow where inertial effects are small, providing stable, efficient runtimes for calibration, whereas the full-momentum variants are preferable where hydraulic controls or rapidly varied flow dominate [49,50]. In addition, the diffusion wave formulations have been widely and successfully applied in floodplain inundation studies [27,45].

ii) Boundary Conditions (BCs)

a. Normal depth

The normal depth boundary inputs the energy slope, which is used to calculate the normal depth with Manning's equation [30]. It is usually estimated using the channel slope. In this study, three (left, right and outlet) boundary condition lines (BCs) were drawn (Figure S3 in Supplementary Materials). To ensure water remains contained within the catchment and does not artificially exit through lateral boundaries, a normal depth slope value of 0 was assigned to the left and right BCs. This setting prevents outflow along these edges by imposing an infinite slope, which HEC-RAS

 doi:10.20944/preprints202512.2831.v1

interprets as a critical depth or free-outfall condition with minimal downstream drawdown effects [51]. For the outlet BC, a value of 0.009 was estimated using Global Mapper Pro v26.0 [52] and adopted.

b. Rainfall Events

In HEC-RAS, rainfall is introduced as a boundary condition to the 2D flow area. The rainfall events used as boundary conditions in this study were selected from the available 15-minute interval rainfall records collected from the Sasscal Automated Station, which is located within the catchment. The rainfall events were selected based on: i) frequent extreme rainfall events since our objective focuses on high flows, ii) availability of corresponding observed hourly flow for model calibration and validation and iii) a period after the implementation of the concrete-lined drainage system in Lusaka to focus on the current conditions. Based on these criteria, three rainfall events shown in Table 3 and Figure 9 were selected. The rainfall event of 9th January 2021 was used for model calibration. In line with best practices in event-based hydrological modelling, particularly in data-scarce contexts, a separate event of 12th January 2022 was selected for validation. The approach involving calibrating the model on one observed flood and validating on a different independent event has been widely applied in HEC-RAS-based flood modelling studies [45,53]. The 29th January 2025 rainfall was selected for scenario analysis to focus on the recent major observed floods in the catchment. In implementing this boundary condition, a uniform rainfall distribution falling over the 2D flow area was assumed since spatial variability in rainfall has a very low impact on the difference in total runoff volume in this particular catchment. This was similarly adopted by other authors, such as Tena et al. [35] who used the WEAP model to develop the water balance of the Chongwe Catchment and Chisola and Kuráž [54] who assessed the patterns of long-term hydrological regime change of the Chongwe River.

Table 3. Rainfall events for calibration, validation and scenario analysis.

Event	Date	Start Time (HH: MM)	End-Time (HH: MM)	Comment
1	09 January, 2021	01:00	09:15	Calibration
2	12 January, 2022	07:45	14:00	Validation
3	29 January, 2025	04:30	09:15	Scenario Analysis

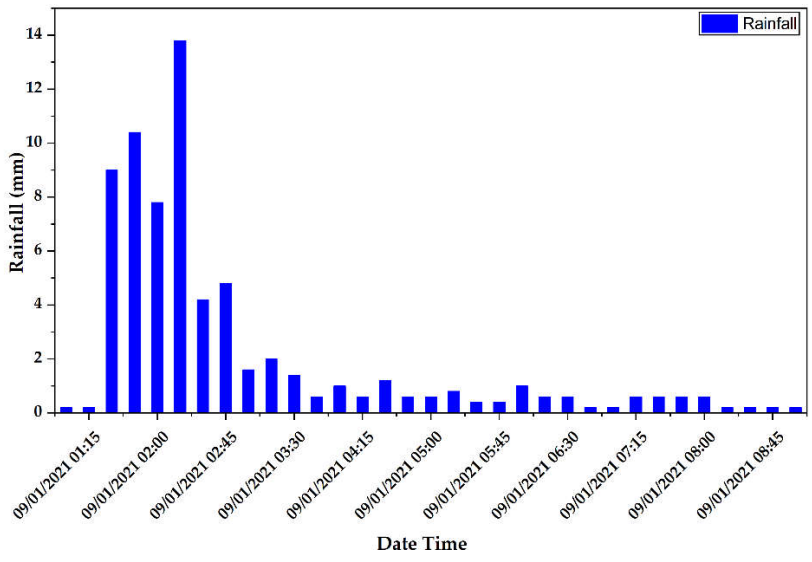

(a)

 doi:10.20944/preprints202512.2831.v1

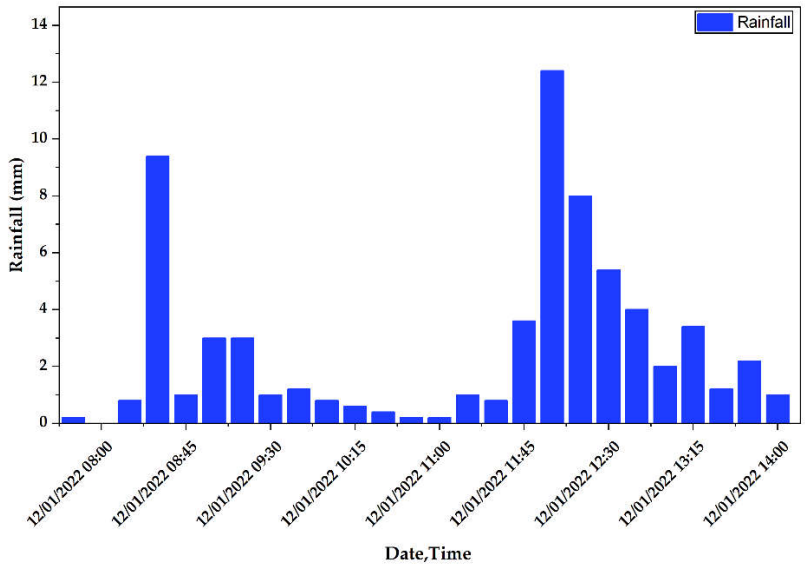

(b)

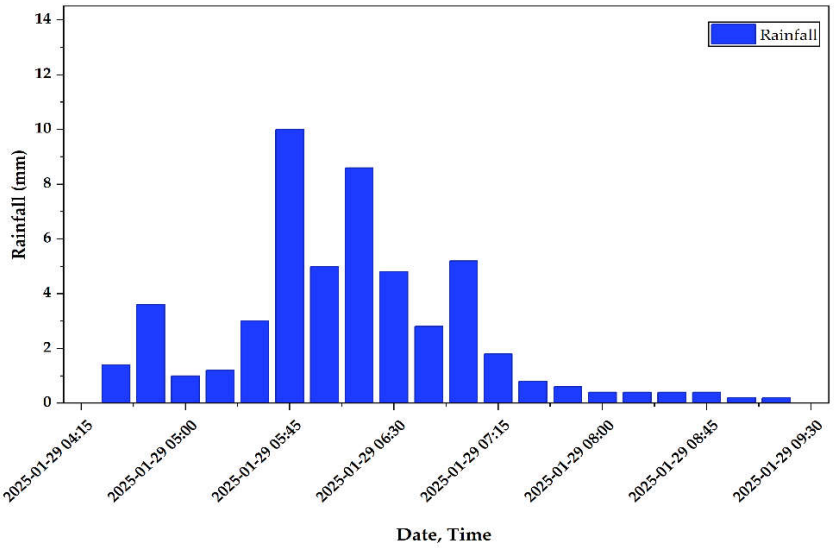

(c)

Figure 9. Rainfall hydrographs for (a) calibration, (b) validation and (c) scenario analysis.

2.4.5. Sensitivity Analysis, Calibration and Validation of HEC-RAS 2D Model

A sensitivity analysis was performed to determine the influence of key model parameters, namely Manning's roughness coefficient, percent impervious, curve number, initial infiltration rate and abstraction ratio, on the peak flow of the Chongwe River as informed by the HECRAS user manual [30]. A local one-factor-at-a-time (OAT) approach was adopted due to the computational cost of 2D simulations and its wide application in flood modelling studies [55]. The initial parameter values assigned from literature [46,47] were systematically perturbed by 20% while all other parameters were held constant to determine their influence on flows at the outlet of the Chongwe Catchment.

To determine the sensitivity of the parameters quantitatively, the Morris OAT method [56] was applied. In this method, the elementary effect (E_i) which represents the change in a selected model output due to a perturbation (Δx_i) of the ith parameter is computed using Equation 6.

$$E_i = \frac{(e_a - e_b)}{\Delta x_i} \quad (6)$$

 doi:10.20944/preprints202512.2831.v1

Where, e_a = the model output after the parameter change, e_b = model output before the change and Δx_i = magnitude of the applied perturbation.

Since, E_i may be positive or negative, depending on the nature of the perturbation, the Morris method uses the absolute mean elementary effect (μ_{i*}) to describe parameter sensitivity, which is computed using Equation 7.

$$\mu_{i*} = \frac{1}{r}\sum_{j=1}^{r} |E_i| \quad (7)$$

Where r is the number of sampling iterations. Due to the computational cost of HEC-RAS 2D simulations, each parameter was evaluated using one perturbation per direction (r = 1) to be consistent with common applications of the Morris OAT method in hydrodynamic modelling [57]. The higher the μ_{i*} value, the more sensitive the parameter [56]. The relative thresholding method [58,59] where μ* values greater than 50% of the maximum are considered high sensitivity, while those below 10% are categorized as low sensitivity, was used to classify the sensitivity of the parameters.

Calibration was performed manually by modifying the sensitive parameters and comparing simulated hydrographs with observed streamflow data at the Great East Road Bridge Gauging Station (RG1) [60]. Validation was subsequently performed using an independent rainfall event to test whether the calibrated model retained its predictive ability without further parameter adjustments. The simulation period for both calibration and validation runs was 48 hours at 15-minute intervals due to HEC-RAS limitations on the number of ordinates for the observed data to conserve computational run-time. The model performance during these runs was evaluated using three performance measures, namely, the coefficient of determination (R^2), the Nash–Sutcliffe Efficiency (NSE), and the Percent Bias (PBIAS). The R^2, NSE, and PBIAS were calculated using Equations 8, 9 and 10, respectively.

$$R^2 = \frac{\left[\sum_{i=1}^{n}(Qo,i-\bar{Q}o)(Qs,i-\bar{Q}s)\right]^2}{\left[\sum_{i=1}^{n}(Qo,i-\bar{Q}o)^2\right]\left[\sum_{i=0}^{n}(Qs,i-\bar{Q}s)^2\right]} \quad (8)$$

$$NSE = 1 - \frac{\left[\sum_{i=1}^{n}(Qo,i-Qs,i)^2\right]}{\left[\sum_{i=0}^{n}(Qo,i-\bar{Q}o)^2\right]} \quad (9)$$

$$PBIAS = 100 \times \frac{\left[\sum_{i=0}^{n}(Qo,i-Qs,i)\right]}{\sum_{i=0}^{n}Qo,i} \quad (10)$$

Where Qo,i = observed discharge at time i, Qs,i = simulated discharge at time i, $\bar{Q}o$ = mean of observed discharges, $\bar{Q}s$ = mean of simulated discharges and n = total number of observations.

It has been documented that i) R^2 is oversensitive to high extreme values, ii) NSE cannot help in identifying model bias and differences in timings and magnitudes, and iii) PBIAS can give a deceiving rating of model performance if the model overpredicts as much as it underpredicts [61]. Therefore, a combination of these performance measures, despite their weaknesses, was adopted in this study to be consistent with their widespread application in hydrological modelling by several authors [34,35,38,62]. The resulting performance statistics were evaluated using the classification criteria for hydrological models (Table 4) recommended by Moriasi et al. [61], similar to the approach followed by [53].

Table 4. Classification criteria for hydrological models [61].

Goodness-of-Fit	NSE	PBIAS (%)	R^2
Very Good (V)	0.75 < NSE ≤ 1.00	PBIAS <±10	$R^2 \geq 0.75$
Good (G)	0.60 < NSE ≤ 0.75	±10 ≤ PBIAS <±15	$0.70 < R^2 \leq 0.75$
Satisfactory (S)	0.50 < NSE ≤ 0.60	± 15 ≤ PBIAS <±45	$0.60 < R^2 \leq 0.75$
Unsatisfactory (U)	NSE ≤ 0.50	PBIAS ≥±45	$R^2 < 0.60$

 doi:10.20944/preprints202512.2831.v1

2.4.6 Simulation of Scenarios represented in the Chongwe Catchment

To evaluate the influence of structural modifications on the hydrological behaviour in the Chongwe River Catchment, four simulation scenarios were designed and executed within the HEC-RAS 2D rain-on-grid framework. These scenarios represent a progression from the current, engineered catchment conditions toward increasingly naturalized states, enabling comparative assessment of the impacts of concrete-lined channels and irrigation dams on runoff generation and peak flow. The description and corresponding model actions applied in each scenario are summarized in Table 5. The results of the scenarios were collected and observed at the outlets of the four sub-catchments.

Table 5. Simulated Scenarios.

Scenario	Name	Description	HEC-RAS Action Tool
1	Current Conditions (Concrete Channels + Dams)	Simulating of catchment as it is with existing 21 km concrete-lined channels and 10 dams	Calibrated model and observed storm
2	Natural Channels + Dams	Simulating the peak flows before concrete-lining of the 21 km of the natural channels in Lusaka, and while observing the effect of dam storage	Adjusting Manning's number of the classification polygons assigned to the concrete-lined channels to natural channels
3	Renaturalization: Natural Channels + No Dams	Simulating the catchment under fully naturalized channels, representing a close to undisturbed channel flow response	Through terrain modification using the channel tool at the dam walls
4	Concrete Channels, No Dams	Simulating a system with concrete-lined channels in Lusaka but without irrigation dams, to highlight the significance of storage in high flow conditions.	Combination of two actions above (2 & 3)

3. Results and Discussion

3.1. Sensitivity Analysis

Sensitivity analysis was conducted using the Morris OAT method on five model parameters by calculating the absolute mean elementary effect (μ_{i*}) after every 48-hour simulation following a parameter perturbation. The results obtained are presented in Table 6. In Morris' OAT sensitivity analysis, the larger the absolute mean elementary effect (μ_{i*}), the more sensitive the parameter is [56]. Therefore, the sensitivity analysis for peak flows in HEC-RAS 2D indicated that Manning's n had by far the largest impact on peak flow, with a much higher μ* value than any other parameter. In contrast, the other parameters, percent impervious, curve number, initial infiltration rate, and abstraction ratio, showed low sensitivity to peak flow. The sensitivity ranking was based on the relative thresholding method classifications presented in Table 7.

The sensitivity analysis results obtained are consistent with other HEC-RAS 2D modelling studies, which also report Manning's n as the dominant factor controlling flood peaks [63,64]. These findings suggest that specifying channel roughness is vital for reproducing peak flow in similar catchments, whereas other surface parameters may have less influence in short-duration flood simulations typical of event-based modelling.

 doi:10.20944/preprints202512.2831.v1

Table 6: Morris (OAT) Sensitivity Analysis Rankings

Parameter	Initial Value (x_i)	Perturbation (Δx_i)	Initial Peak Flow (e_b) (m^3/s)	Perturbed Flow (e_a) (m^3/s)	Ei (r=1)	Absolute Effect (μ_i^*)	Sensitivity Ranking
Manning's n	0.064	0.012	122.760	105.990	– 1,397.500	1,397.500	Very High
% Impervious	16.000	3.200	122.760	145.89	+7.230	7.230	Low
Curve Number	86.310	10.090	122.760	386.400	+ 26.140	26.140	Low
Initial Infiltration Rate (mm/hr.)	1.300	0.260	122.760	117.080	–21.850	21.850	Low
Abstraction Ratio	0.200	0.04	122.760	110.580	–30.500	30.500	Low

Table 7. Relative threshold criteria for classifying parameter sensitivity [59].

μ* Range (Relative to Max)	Sensitivity Classification
$\mu^* > 700$	Very High
$150 < \mu^* \leq 700$	High
$50 < \mu^* \leq 150$	Moderate
$\mu^* \leq 50$	Low

3.2. Model Calibration and Validation

The HEC-RAS 2D model was calibrated over a simulation period of 48 hours following a 15-minute interval rainfall event using Manning's n and percent impervious for the hydraulic face properties under LULC classes and curve number, initial infiltration rate and abstraction rate under the infiltration layer. Table 8 presents the initial and calibrated Manning's n and percent impervious values (Land cover layer parameters), while Table S2 in the supplementary material presents the initial and calibrated values of curve number, initial infiltration rate and abstraction rate assigned to the infiltration layer.

Table 8. Initial and calibrated Manning's n & % impervious values.

	LULC Class	Manning's n		Percent Impervious %)	
ID	Name	Initial	Calibrated	Initial	Calibrated
1	Shrubland	0.100	0.120	2.000	2.000
3	Built-up Land	0.045	0.030	70.000	85.000
4	Grassland	0.060	0.055	5.000	5.000
5	Cropland	0.050	0.050	2.000	3.000
6	Barren Land	0.040	0.030	0.000	0.000
7	Wetland	0.120	0.120	0.000	0.000
8	Open Water	0.025	0.025	0.000	0.000
10	Forest	0.120	0.160	1.000	1.000
9	Natural Channel	0.035	0.035	1.000	1.000
2	C* Drain	0.013	0.013	1.000	100.000

*Concrete-lined drainage channels

 doi:10.20944/preprints202512.2831.v1

A graphical comparison of the simulated flow and the observed flow at the outlet of the Chongwe Catchment, shown in Figure 10, shows a good model prediction of the observed flow. The statistical computations of model performance during calibration were also conducted, in which R^2, NSE and PBIAS were found to be 0.99, 0.75 and –0.68 % respectively. The R^2 value of 0.99 indicates that the model closely followed the overall temporal pattern of the hydrograph, capturing the trends of flood [65]. The NSE value of 0.75 obtained shows that the model reproduced observed flow magnitudes with reasonable accuracy, though it also suggests moderate discrepancies during peak flows [61]. The negative value of PBIAS indicates that the model overestimated the peak flows [65]; however, all the results of statistics obtained fall within the good to very good thresholds defined by Moriasi et al. [61].

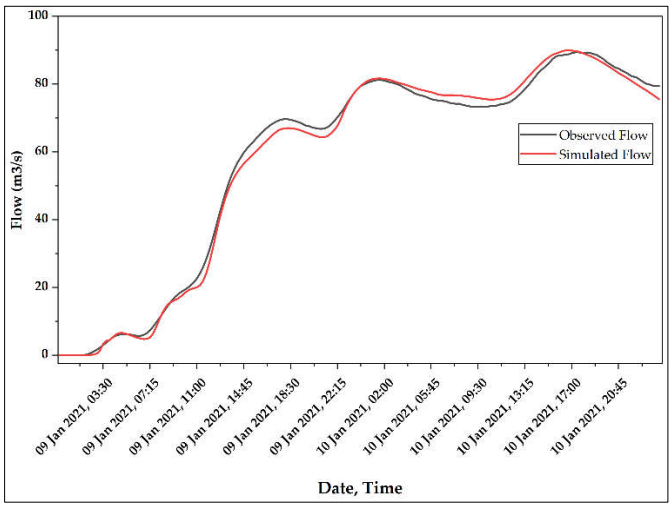

Figure 10. Sub-hourly (15-min) flow calibration results for gauging station RG1 located at Great East Road Bridge.

The calibrated model parameters were used for the validation of flow using an independent rainfall event which occurred on 12th January, 2022 and the corresponding observed flow event and the results are presented in Figure 11. The validation exercise achieved R^2, NSE and PBIAS of 0.95, 0.75, and –2.49 % respectively. R^2 and NSE were similar to calibration results; however, PBIAS shows that the model further overestimated the peak flows during validation compared to calibration. Overall, the HEC-RAS 2D simulations seem to capture the observed flow well both during calibration and validation runs based on the recommendations of Moriasi et al. [61].

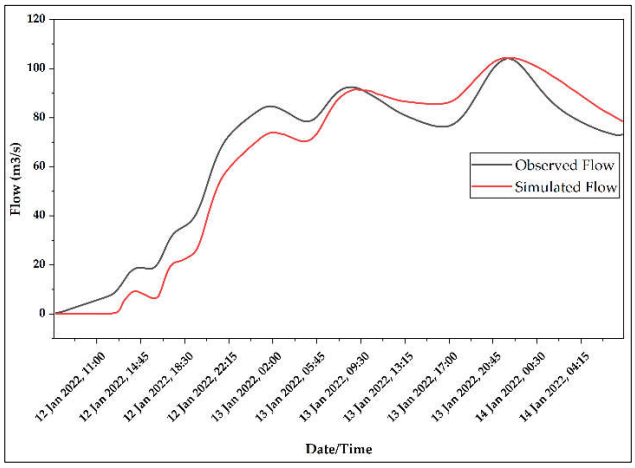

Figure 11. Sub-hourly (15-min) flow validation results for gauging station RG1 located at Great East Road Bridge.

 doi:10.20944/preprints202512.2831.v1

3.3. Effects of Concrete-Lining of Natural Channels on High Flows

To segregate the hydrological effects of urban channel modification, Scenario 3, which represents a naturalized condition with unlined channels and no dam, was used as the baseline for comparison. Scenario 4 simulates the same catchment but with 21 km of urban headwater channels of the Ngwerere River in Lusaka replaced by a concrete-lined drainage channel. The difference between these two scenarios captures the impact of concrete-lining on the hydrological response. The results showed that concrete-lining of 21 km of urban headwater channels significantly altered flood flows at the outlet of the Ngwerere sub-catchment, where urban drainage upgrades were implemented. A comparison between Scenario 3 (natural channels, no dams) and Scenario 4 (concrete-lined channels, no dams) showed that peak flow increased by 11% (from 49.44 m^3/s to 54.91 m^3/s), flood depth rose from 3.79 m to 3.88 m and flood extent expanded from 114 m to 117 m. Lag time decreased by 12 minutes, indicating faster runoff concentration. These changes are presented in Figure 12 and Table 9.

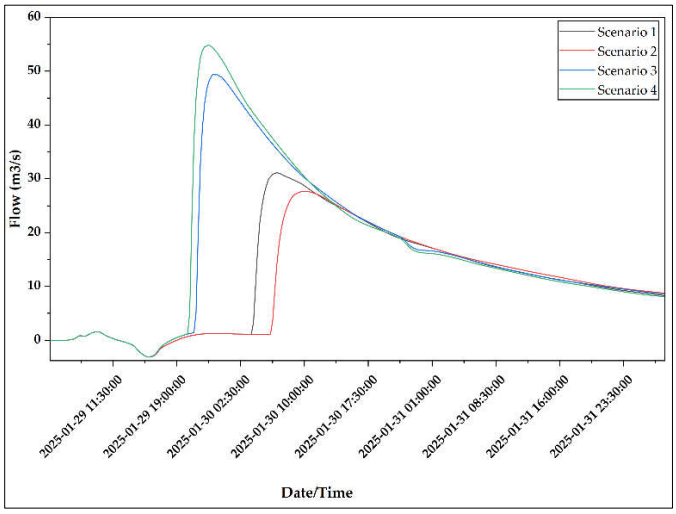

Figure 12. High flow characteristics at the Ngwerere outlet for different scenarios.

Table 9. Summary of Flow Characteristics at Ngwerere Outlet for the four scenarios.

Scenario	Peak Flow (m^3/s)	Lag-time (hr.)	Maximum Flood Depth (m)	Flood extent (m)
1	31.14	25.00	3.44	110.00
2	27.72	28.15	3.37	105.00
3	49.44	17.30	3.79	114.00
4	54.91	17.50	3.88	117.00

Historically, flooding has been a recurrent problem in Lusaka due to rapid urban expansion, encroachment into floodplains and inadequate stormwater drainage infrastructure [38,66]. Prior to the concrete-lining of natural urban channels, flood events were frequently reported during rainfall, causing damage to roads, informal settlements, and public infrastructure [66]. These challenges prompted the adoption of channel-lining as a means of rapidly conveying stormwater through densely urbanized areas [31]. However, while channel concrete-lining improves flow conveyance within modified reaches, it also fundamentally alters natural flow resistance. Therefore, the observed increases in peak flow and flood extent can be attributed to the **reduction in channel surface roughness** and the **lack of natural detention** associated with concrete-lining. Natural channels typically slow flow through resistance provided by vegetation and irregular geometry and they also facilitate infiltration and temporary storage [67]. In contrast, concrete-lined channels are

 doi:10.20944/preprints202512.2831.v1

hydraulically efficient, allowing rapid flow conveyance while limiting infiltration and subsurface storage interactions [19]. This is supported by the results shown in Figures 13 and 14, in which the velocity outputs across the concrete-lined main drainage channel were extracted for both the concrete-lined and natural channel scenarios and compared. The results showed that in the concrete-lined channels, maximum velocities increased and ranged between approximately 8 m/s and 20 m/s across the channel width. In the natural channel scenario, maximum velocities were lower than 5 m/s.

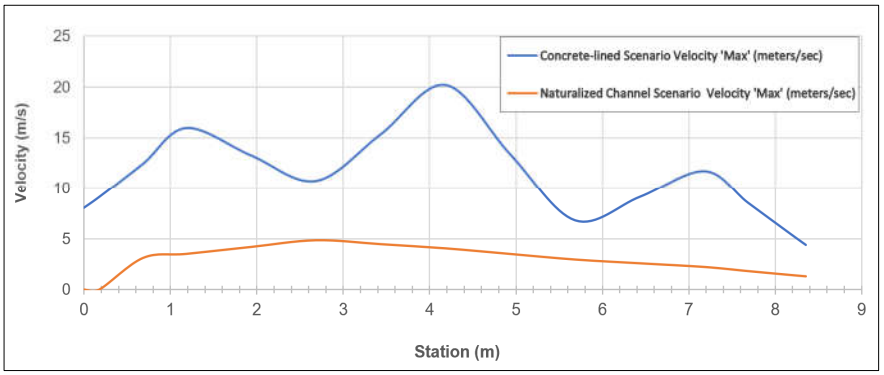

Figure 13. Comparison of velocity in a naturalized channel and a concrete-lined channel at Kasangula Road Bridge (KRB).

Similar hydrological responses to concrete-lining have been reported in other highly urbanized catchments. For example, in the Bukit Timah catchment in Singapore, Palanisamy and Chui[68] showed that concrete-lined drainage canals increased runoff volumes contributing to downstream flood risk. Their study demonstrated that such hydraulic efficiency necessitates complementary mitigation measures, such as low-impact development techniques to restore infiltration and reduce peak flows. Beyond hydrological impacts, studies in other urban catchments have shown that concrete drainage infrastructure can also alter runoff water quality through geochemical interactions between stormwater and concrete surfaces. For example, Wright et al. [69], based on observations from urban catchments in Melbourne, Australia, reported elevated pH, alkalinity, and calcium concentrations in streams receiving runoff conveyed through concrete-lined drainage systems. This suggests that, in addition to increased flood magnitudes downstream, concrete-lining in the Chongwe Catchment may also have implications for runoff quality and stream health, necessitating further investigation in future studies.

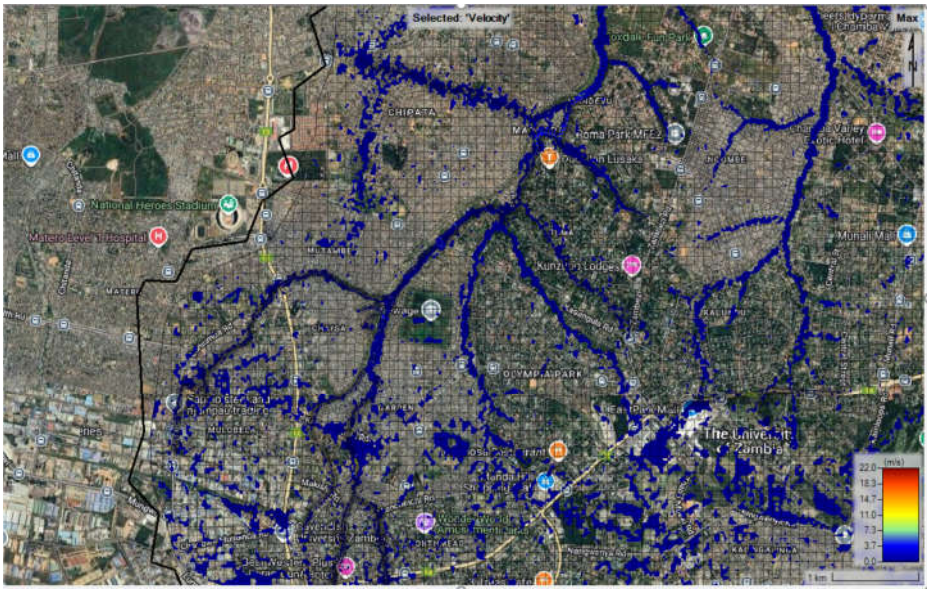

(a)

 doi:10.20944/preprints202512.2831.v1

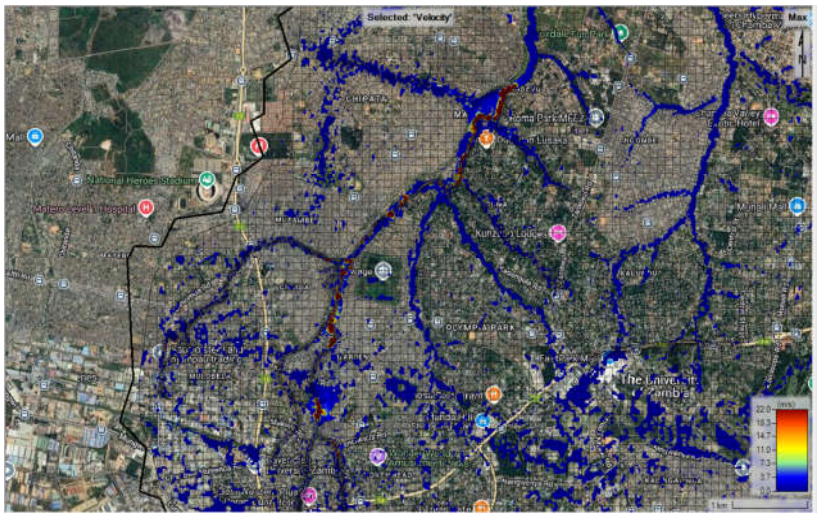

(b)

Figure 14. Comparison of maximum velocities along: (a) Naturalized channel (Scenario 3) and (b) Concrete-lined channel (Scenario 4) in Lusaka.

The observed increase in velocity in the concrete-lined channel can be explained by Manning's equation which relates velocity to the roughness coefficient, channel slope, and hydraulic radius [70]. When the Manning's n value is lowered, the flow experiences less frictional loss and accelerates accordingly. Moreover, the smoother surface eliminates micro-pooling and surface storage that would otherwise reduce momentum. Furthermore, concrete channels are often more directly connected to impervious urban surfaces, which increases both the velocity and volume of runoff entering the drainage channel system. As a result, the flow becomes more concentrated, contributing to elevated flood levels and wider flood inundation extents at the catchment outlet.

At the main Chongwe River outlet, the downstream influence of upstream concrete-lining was also evident, although the magnitude of hydrological changes was less pronounced. Comparing Scenario 4 (concrete-lined, no dams) with Scenario 3 (natural channels, no dams) at the main outlet of the Chongwe River showed that peak flow increased by 4.6% from 73.60 m^3/s to 77.00 m^3/s (Figure 15). Lag time decreased by approximately 75 minutes, indicating that urban channel modifications in the Ngwerere sub-catchment accelerated the arrival of the flood wave downstream. The maximum flood depth increased slightly from 1.99 m to 2.22 m, while the flood extent expanded from 102 m to 104 m. The spatial differences in flood depth distribution and inundation extent along the Chongwe outlet reach are illustrated in Figures 16 and 17, respectively. The quantitative changes are summarized in Table 10.

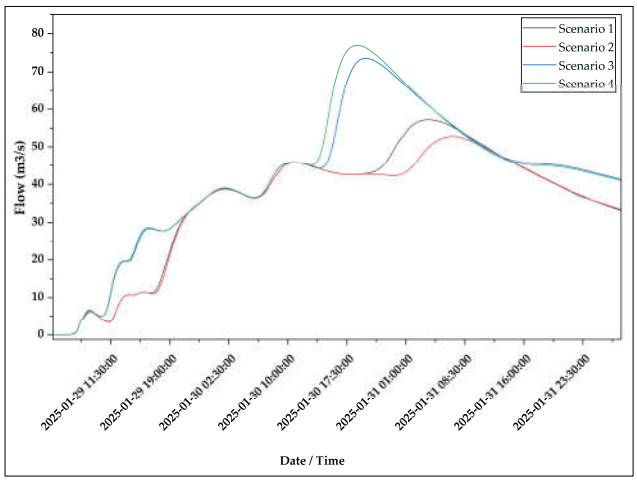

Figure 15. Summary of Flow Characteristics at Chongwe main outlet for the four scenarios.

 doi:10.20944/preprints202512.2831.v1

.

Table 10. Summary of Flow Characteristics at Chongwe main outlet for the four scenarios.

Scenario	Peak Flow (m^3/s)	Lag-time (hr.)	Maximum Flood Depth (m)	Flood extent (m)
1	57.25	46.00	1.81	100.00
2	52.82	49.25	1.77	98.00
3	73.60	38.25	1.99	102.00
4	77.00	37.00	2.22	104.00

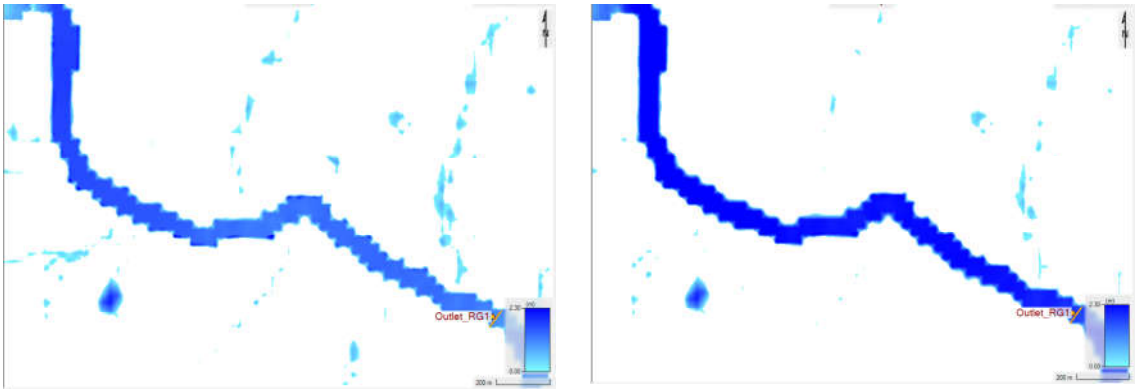

(a) (b)

Figure 16. Comparison of maximum flood depth distribution in RAS Mapper at the Chongwe River (RG1) Reach under (a) natural channel conditions without concrete-lining (Scenario 3) and (b) concrete-lined channel conditions in Lusaka City (Scenario 4).

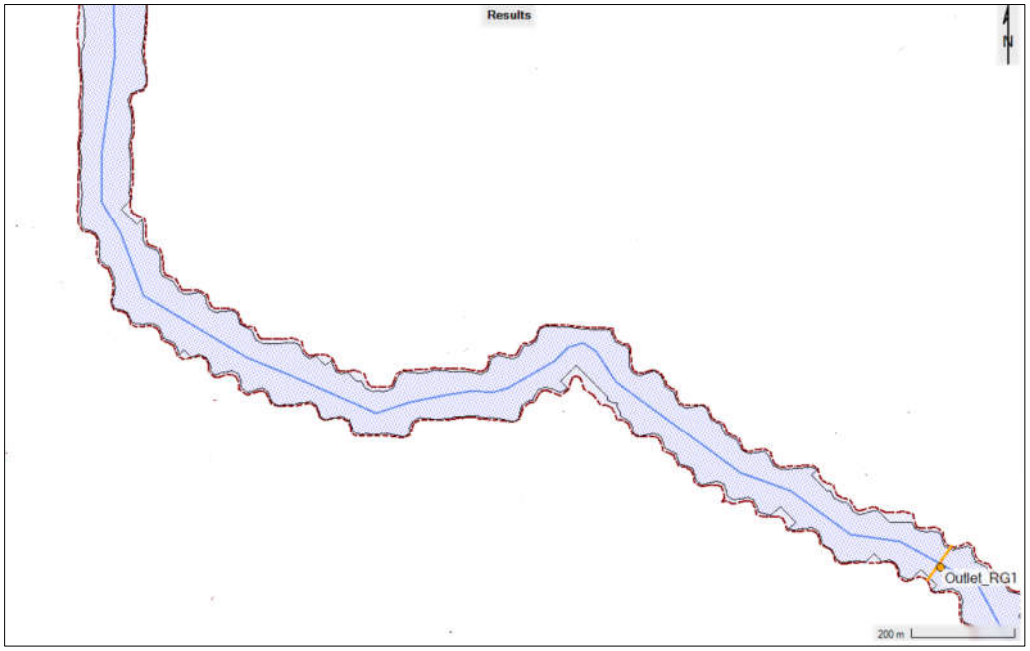

Figure 17. Overlay comparison of flood inundation boundaries in RAS Mapper at the Chongwe River Outlet (RG1) Reach for Scenario 3 (natural channels, shown by the black solid line) and Scenario 4 (concrete-lined channels, shown by the red dashed line).

 doi:10.20944/preprints202512.2831.v1

The simulated downstream changes in the high flows (Figure 15) suggest that even localized structural modifications, such as concrete-lining within a single urban sub-catchment, can have cascading effects at the catchment scale. The accelerated routing of stormwater reduces the time available for the natural hydrological processes, thereby increasing the timing and extent of downstream flooding. This effect is further reflected in the flood depth and inundation maps (Figures 16 and 17), where concrete-lined channels are associated with increased flow movement leading to increases in flood depth and inundation extent at the Chongwe River outlet reach. These findings highlight the importance of considering system-wide hydrologic connectivity when designing urban drainage interventions. Our findings are consistent with studies such as Ress et al. [6] who reported increased peak flows when natural channels are replaced by engineered stormwater drainage systems. While these findings are out of a 15-minute interval rainfall event-based modelling, they support the findings of Chisola and Kuráž [54] who analyzed long-term streamflow time-series and reported an increase in streamflow during wet seasons and a reduction in dry season, suggesting a decrease in lag time, similar to our results. Tena et al. [38] attributed rising wet-season flows to the rapid expansion of buildings and road infrastructure in Lusaka. Our study adds new evidence by showing that the observed increases in flow in wet seasons may further be linked to the construction of the 21 km concrete-lined drainage system (the Bombay drain) in Lusaka, which enhances runoff concentration and accelerates peak-flow delivery to the Chongwe River.

3.4. Effects of dam storage on High-flows

To evaluate the effects of dam storage on high flows, Scenario 2 (natural channels with dams) was compared with Scenario 3 (natural channels without dams) at the outlets. This comparison isolates the hydrological influence of existing irrigation and water supply dams while keeping the surface channel characteristic constant. In addition, dam-related simulations were conducted assuming low initial reservoir levels at the onset of the rainfall event, representing near-empty storage conditions to isolate the effect of dam storage under conditions of maximum available capacity [71]. This assumption is justified because the majority of existing dams in the Chongwe Catchment are small and are frequently observed to contain little water or to be in a dry state, particularly outside periods of sustained rainfall due to over-abstraction [54,72].

The results showed that dam presence reduced peak flows and delayed flood wave propagation across the Chongwe River Catchment. At the Ngwerere outlet, peak flow decreased by 44%, from 49.44 m^3/s in Scenario 3 to 27.72 m^3/s in Scenario 2. Lag time increased by approximately 11 hours, from 17.05 to 27.93 hours, while flood depth and extent decreased by 11% and 8%, respectively (Figure 12 and Table 9). These changes can be attributed to the presence of the Kasisi Dam on the Ngwerere River, which stores stormwater and thus delays and reduces downstream flow volumes. The dams temporarily store inflowing stormwater during peak rainfall periods and release it gradually through outlet structures [73]. If a comparable rainfall event were to occur when the reservoirs are already at or near full supply level, the available storage for flood attenuation would be substantially reduced and a greater proportion of inflowing floodwaters would be routed downstream, resulting in increased peak discharge, reduced lag time, and enhanced downstream flood depths and inundation extent [74].

A similar pattern was observed at the Upper Chongwe outlet, where the presence of upstream dams reduced high-flow magnitudes. Peak flow decreased by 35%, from 14.73 m^3/s under Scenario 3 (no dams) to 9.64 m^3/s under Scenario 2 (with dams), as shown in Figure 18 and Table 11. In addition, the maximum flood depth decreased from 1.71 m to 1.52 m, while flood extent contracted from 89 m to 80 m, demonstrating the capacity of upstream storage to reduce flood levels and downstream flood inundation. However, the response in lag time differed from other sub-catchments. Lag time shortened substantially from 56.45 hr. in the no-dam scenario to 13 hr. when dams were present. This contrasting behaviour reflects the proximity of seven dams, including the largest (Ray Dam), to the outlet. Under dam-present conditions, flows reaching the outlet are dominated by spillway releases and outflows that respond more rapidly once reservoir levels rise. When the dam is removed in the

 doi:10.20944/preprints202512.2831.v1

simulation, inflows must travel the entire natural channel system, resulting in longer flood-wave travel times. Under full-reservoir conditions, spillway-controlled outflows would be initiated earlier and convey higher downstream discharges, thereby diminishing the flood-attenuation benefits observed under the low initial reservoir conditions assumed in this study.

This finding is similar to the findings of Olariu et al. [75] in the Siret River Basin, who demonstrated that the influence of dams is strongest closest to the dam, then decreases downstream as the river system recovers its natural state. Therefore, the hydrograph is dominated by spillway releases rather than natural channel routing. This finding calls for the need for multiple hydrograph observation points along the river; otherwise, near-dam outlets observations only can give a misleading picture of catchment response in structurally modified basins [76].

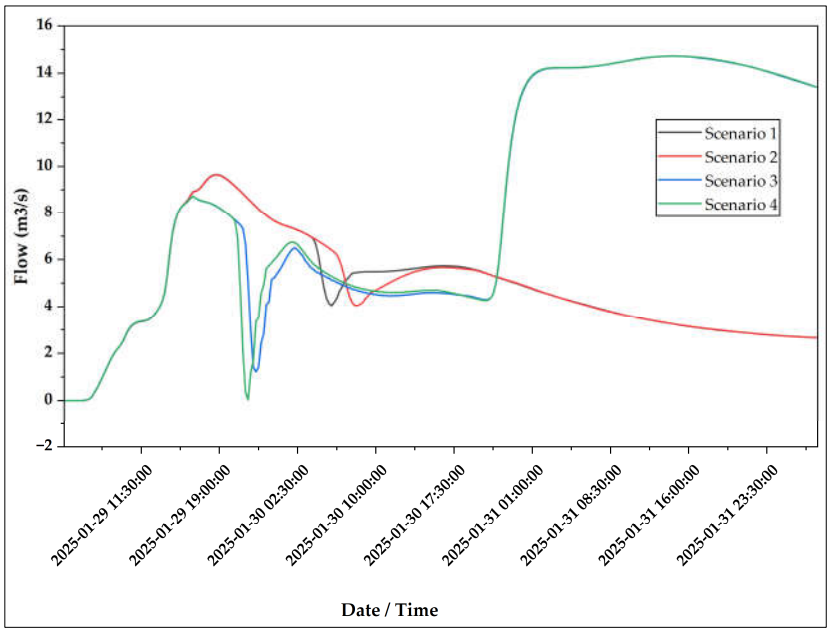

Figure 18. High flow characteristics at the Upper Chongwe outlet for different scenarios.

Table 11. Summary of Flow Characteristics at Upper Chongwe Outlet for the four scenarios.

Scenario	Peak Flow (m^3/s)	Lag-time (hr.)	Maximum Flood Depth (m)	Flood extent (m)
1	9.65	13.00	1.15	101.00
2	9.64	13.00	1.11	97.00
3	14.73	56.45	1.50	105.00
4	14.74	57.00	1.59	108.00

At the Main Chongwe outlet, the combined effect of all the 10 upstream dams produced a 28% reduction in peak flow from 73.60 m^3/s (Scenario 3) to 52.82 m^3/s (Scenario 2). Lag time increased from 38.25 hours to 49.25 hours, a 29% delay in flood wave arrival at the outlet. The maximum flood depth decreased by 11% and the flood extent narrowed by 4% (Figure 15, Table 10). These results show that 10 dams across the Chongwe Catchment play a substantial role in attenuating extreme flow events under short-duration, high-intensity rainfall. While previous assessments in the catchment have focused primarily on monthly or annual streamflow trends [38,77], our event-based simulation reveals the sub-hourly effects of dam infrastructure on high-flow regulation. The findings suggest that current dams provide effective mitigation of flash flood peaks and that their hydrological influence is both location-dependent and event-specific.

 doi:10.20944/preprints202512.2831.v1

3.5. Integrated Effects of Concrete-lining of Natural Channels and Dam Storage

The integrated effects of urban concrete-lining and dam storage were assessed by comparing Scenario 1 (concrete-lined channels with existing dams) against the naturalized Scenario 3. This comparison captures the effect of structural modifications introduced for flood management in the Chongwe Catchment. At the Ngwerere outlet, peak flow decreased by 43%, from 54.91 m^3/s in Scenario 3 to 31.14 m^3/s in Scenario 1. Flood depth dropped by 11% from 3.88 m to 3.44 m and flood extent narrowed by 6% from 117 m to 110 m. Lag time increased by 43% suggesting a delayed runoff response despite the presence of the 21km of concrete-lined drains in Lusaka. These changes can be attributed to the presence of the Kasisi Dam on the Ngwerere River, which stores stormwater, thereby reducing peak flows influenced by concrete-lined channels.

At the Main Chongwe outlet, the integrated influence of structural measures was similarly evident (Figure 15 and Table 10). Peak flow decreased from 76.99 m^3/s (Scenario 3) to 57.25 m^3/s (Scenario 1), representing a 26% reduction. Lag time increased by 24%, while flood depth and flood extent reduced by 10% and 4%, respectively. The overlay comparison of the flood inundation boundaries depicting the integrated influence of concrete-lining and dams is shown in Figure 19. These results reflect the cumulative regulating effect of multiple dams situated in the Ngwerere, Upper Chongwe and Lower Chongwe sub-catchments which capture and store water over time and thus lessen the flood wave arriving at the outlet [73]. It should be noted that if similar rainfall events were to occur under full-reservoir conditions, the flood storage effects would be reduced, resulting in higher peak flows, shorter lag times and increased flood depth and inundation extent as spillway-controlled outflows become dominant [74].

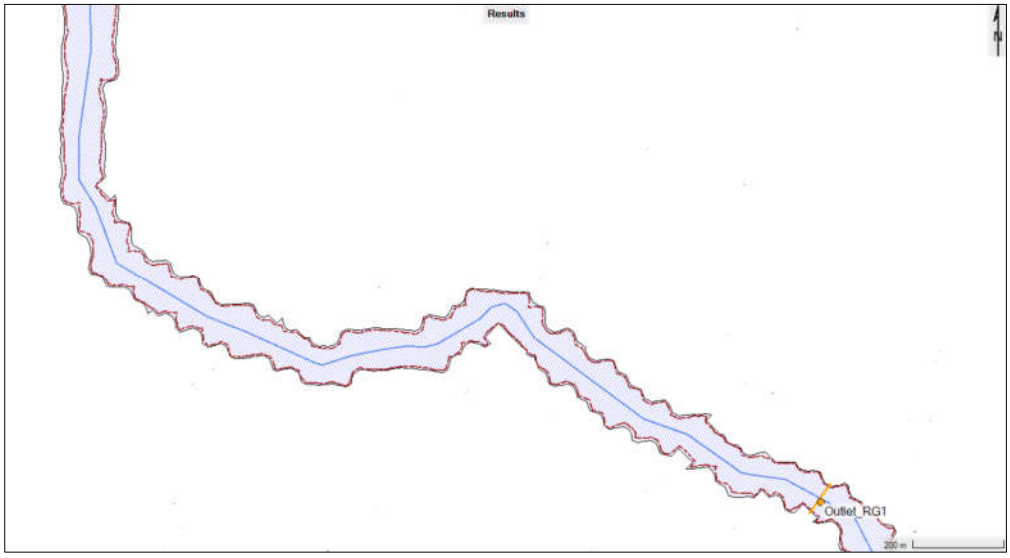

Figure 19. Overlay comparison of flood inundation boundaries in RAS Mapper at the Chongwe River (RG1) Reach for Scenario 3 (natural channels, shown by the black solid line) and Scenario 1 (concrete-lined channels with dams shown by the brown dashed line).

The overall hydrological behaviour across all four scenarios demonstrated that although concrete-lining alone tends to accelerate and increase flow magnitudes, dam storage counteracts these effects by storing some volume of the flow [78]. This hydraulic buffering effect is supported by previous studies [79,80] which demonstrate that dams reduce both the magnitude and timing of peak flows, particularly when positioned close to areas of rapid runoff generation. Despite these reductions, flow velocities within the concrete-lined sections remained high, ranging from 8 to 20 m/s, far exceeding those recorded under natural-channel conditions. This presents a continued risk of downstream erosion and structural damage, even when peak volumes are reduced downstream. This underscores the need for a hybrid flood management approach which includes Nature-based Solutions (NbS) such as vegetated swales, wetlands and green spaces to reduce flow velocity, enhance

 doi:10.20944/preprints202512.2831.v1

infiltration, and increase catchment resilience. Integrating NbS alongside existing hard infrastructure may offer a more sustainable solution to managing urban flood risks in rapidly developing catchments like Chongwe [16].

4. Conclusions and Recommendations

This study used a 2D rain-on-grid HEC-RAS event-based modelling approach to evaluate the influence of concrete-lining of natural channels and dam storage on high-flow behaviour in the Chongwe River Catchment. The model performed well with $R^2 = 0.99$, NSE = 0.75, and PBIAS = – 0.68 % for calibration, and $R^2 = 0.95$, NSE = 0.75, and PBIAS = – 2.49 % for validation. This shows that the model is suitable for event-based flood modelling in the Chongwe Catchment and similar catchments. The study demonstrated that the concrete-lining of 21 km of natural drainage channels in Lusaka increased high flows by approximately 4.6% at the main catchment outlet and generated very high flow velocities within the urban drainage system. On the other hand, the 10 existing dams reduced peak flows by about 28% and increased lag times by 24%, while flood depth and flood extent reduced by 10% and 4%, respectively. This demonstrates their important role in reducing the magnitude of flash floods. Future urban planning should incorporate downstream storage infrastructure such as dams, alongside major drainage upgrades to effectively capture stormwater and mitigate the high-flow impacts associated with the concrete-lining of natural channels. Additionally, literature has shown that concrete-lining of natural channels in urban areas can affect the runoff water quality through geochemical interactions between stormwater and concrete surfaces. Therefore, planning efforts should holistically consider both quantity and quality aspects to ensure that downstream water bodies, including dams, maintain acceptable water quality standards for domestic and agricultural use.

The limitations of the study include: (i) the use of event-based simulation rather than continuous long-term modelling, which does not capture seasonal hydrological variability or dam operation dynamics; (ii) simplified river channel representation due to sparse cross-section data and manual interpolation, which may introduce geometric uncertainty in modified channels and dam structures; and (iii) the assumption of uniform rainfall distribution across the catchment, which may overlook spatial rainfall variability during localized storms. Future research could also benefit from continuous modelling over longer periods to quantify the effects of dams under a wider range of hydrometeorological conditions. For sub-catchments such as Kanakantapa, where no significant structural modifications were observed but rain-fed agriculture is predominant [34], further assessment of land management and soil conditions is needed to guide the selection of suitable interventions across the Chongwe River Catchment.

Supplementary Materials: The following supporting information can be downloaded at: https://www.mdpi.com/article/doi/s1, Table S1: Cross-Sections and Elevations; Figure S1: Sample Terrain Modification; Figure S2: 2D Flow Area Characteristics; Figure S3: SCS Curve Number Method Input Parameters; Figure S4: Three Normal Depth Boundary Lines Regulating Flow Out of The Catchment; Figure S5: Computational Summaries of the Four Scenario Run

Author Contributions: F.M. designed the methodology, performed the modelling and analysis, interpreted the results, and prepared the original draft of the manuscript. H.M., J.M.G., and C.W.M. supervised the research and design of the methodology, provided guidance throughout the modelling and interpretation stages, and contributed to the review and editing of the manuscript. All authors have read and agreed to the published version of the manuscript.

Funding: This work is supported financially by the German Academic Exchange Service (DAAD) Organisation through the "DAAD In-Country In-Region Scholarship Programme - Kenya, JKUAT SWEED - PhD, 2023 programme. Cohort 1". The opinions expressed are those of the author and do not necessarily represent the policy of the German Academic Exchange Service (DAAD).

 doi:10.20944/preprints202512.2831.v1

Data Availability Statement: Data is contained within the article, or supplementary material; however, the model files developed can be obtained from the corresponding author upon reasonable request.

Acknowledgments: This work was made possible by the financial and academic support of the German Academic Exchange Service (DAAD) and the Jomo Kenyatta University of Agriculture and Technology (JKUAT), whose support is acknowledged with thankfulness.

Conflicts of Interest: The authors declare no conflicts of interest.

Abbreviations

2D	Two-Dimensional
ADCP	Acoustic Doppler Current Profiler
OAT	One-factor-At-a-Time
DAAD	German Academic Exchange Service
DEM	Digital Elevation Model
DMC	Double-Mass Curve
DWRD	Department of Water Resources Development
ELM	Eulerian–Lagrangian Method
ESA	European Space Agency
FAO	Food and Agriculture Organization
HSG	Hydrologic Soil Group
HEC-RAS	Hydrologic Engineering Center – River Analysis System
HEC-HMS	Hydrologic Engineering Center – Hydrologic Modeling System
IDF	Intensity–Duration–Frequency
JAXA	Japan Aerospace Exploration Agency
JKUAT	Jomo Kenyatta University of Agriculture and Technology
LCC	Lusaka City Council
LID	Low Impact Development
LULC	Land Use/Land Cover
NSE	Nash–Sutcliffe Efficiency
NbS	Nature-Based Solutions
PBIAS	Percent Bias
PRISM	Panchromatic Remote-Sensing Instrument for Stereo Mapping
QGIS	Quantum Geographic Information System
RAS	River Analysis System
RG1	Great East Road Bridge Gauging Station
SASSCAL	Southern African Science Service Centre for Climate Change and Adaptive Land Management
SCS	Soil Conservation Service
SWE	Shallow Water Equations
SWE-EM	Shallow Water Equations – Explicit Momentum
SWE-LIA	Shallow Water Equations – Local Inertia Approximation
USACE	United States Army Corps of Engineers
WARMA	Water Resources Management Authority
WEAP	Water Evaluation And Planning System
ZMD	Zambia Meteorological Department

 doi:10.20944/preprints202512.2831.v1

References

1. IPCC. Climate Change 2022 – Impacts, Adaptation and Vulnerability. Contribution of Working Group II to the Sixth Assessment Report of the Intergovernmental Panel on Climate Change [H.-O. Pörtner, D.C. Roberts, M. Tignor, E.S. Poloczanska, K. Mintenbeck, A. Alegría, M. Craig, S. Langsdorf, S. Löschke, V. Möller, A. Okem, B. Rama (eds.)]. Cambridge University Press; 2022. https://doi.org/10.1017/9781009325844.
2. Li Z, Li W, Li Z, Lv X. Responses of Runoff and Its Extremes to Climate Change in the Upper Catchment of the Heihe River Basin, China. Atmosphere (Basel) 2023;14. https://doi.org/10.3390/atmos14030539.
3. Gray LC, Zhao L, Stillwell AS. Impacts of climate change on global total and urban runoff. J Hydrol (Amst) 2023;620. https://doi.org/10.1016/j.jhydrol.2023.129352.
4. National Geographic Society. The Influence of Climate Change on Extreme Environmental Events. Https://EducationNationalgeographicOrg/Resource/Influence-Climate-Change-Extreme-Environmental-Events/ 2023.
5. Dunn SM, Mackay R. Modelling the hydrological impacts of open ditch drainage. vol. 179. 1996.
6. Ress LD, Hung CLJ, James LA. Impacts of urban drainage systems on stormwater hydrology: Rocky Branch Watershed, Columbia, South Carolina. J Flood Risk Manag 2020;13. https://doi.org/10.1111/jfr3.12643.
7. Gao Y, Sarker S, Sarker T, Leta OT. Analyzing the critical locations in response of constructed and planned dams on the Mekong River Basin for environmental integrity. Environ Res Commun 2022;4:101001. https://doi.org/10.1088/2515-7620/ac9459.
8. Natarajan S, Radhakrishnan N. An Integrated Hydrologic and Hydraulic Flood Modeling Study for a Medium-Sized Ungauged Urban Catchment Area: A Case Study of Tiruchirappalli City Using HEC-HMS and HEC-RAS. Journal of The Institution of Engineers (India): Series A 2020;101:381–98. https://doi.org/10.1007/s40030-019-00427-2.
9. Onchi-Ramos K, Rodríguez-Cuevas C, Couder-Castañeda C, Padilla-Pérez DA. Flood Risk Assessment of the Garita River in the Urban Zone of San Luis Potosí City, by Hydrodynamic Modeling. Sci Rep 2024;14. https://doi.org/10.1038/s41598-024-66743-1.
10. Kanema EM, Gumindoga W. Effects of changing climate on the groundwater potential: A case of Chongwe and Rufunsa Districts along the Chongwe River Catchment, Zambia. Physics and Chemistry of the Earth 2022;127. https://doi.org/10.1016/j.pce.2022.103192.
11. Zainal NN, Abu Talib SH. Review paper on applications of the HEC-RAS model for flooding, agriculture, and water quality simulation. Water Pract Technol 2024;19:2883–900. https://doi.org/10.2166/wpt.2024.173.
12. Zhao B, Xin T, Li P, Ma F, Gao B, Fan R. Regulation of Flood Dynamics by a Check Dam System in a Typical Ecological Construction Watershed on the Loess Plateau, China. Water (Basel) 2023;15:2000. https://doi.org/10.3390/w15112000.
13. Mwelwa D, Mwaanga P, Nguvulu A, Tena TM, Taye G. Assessment of catchment water resources allocation under climate change in Luwombwa sub-catchment, Zambia. Heliyon 2024;10. https://doi.org/10.1016/j.heliyon.2024.e39962.
14. Mwelwa D, Tena TM, Nguvulu A, Mwaanga P, Taye G. Surface water availability in ungauged catchments of Sub-Saharan Africa: A case study from Luwombwa sub-catchment, Zambia. Water Science 2025;39:42–57. https://doi.org/10.1080/23570008.2024.2439586.
15. Huang S, Gan Y, Chen N, Wang C, Zhang X, Li C, et al. Urbanization enhances channel and surface runoff: A quantitative analysis using both physical and empirical models over the Yangtze River basin. J Hydrol (Amst) 2024;635:131194. https://doi.org/10.1016/j.jhydrol.2024.131194.
16. Mudenda F, Mwangi H, Gathenya JM, Maina CW, Tena TM. Structural and nature-based solutions for resilient watershed systems: a systematic review of watershed modelling approaches and global datasets. Journal of Water and Climate Change 2025. https://doi.org/10.2166/wcc.2025.814.
17. Tena TM, Nguvulu A, Mwelwa D, Mwaanga P. Assessing Water Availability and Unmet Water Demand Using the WEAP Model in the Semi-Arid Bweengwa, Kasaka and Magoye Sub-Catchments of Southern Zambia. J Environ Prot (Irvine, Calif) 2021;12:280–95. https://doi.org/10.4236/jep.2021.124018.
18. Rose S, Peters NE. Effects of urbanization on streamflow in the Atlanta area (Georgia, USA): a comparative hydrological approach. Hydrol Process 2001;15:1441–57. https://doi.org/10.1002/hyp.218.

 doi:10.20944/preprints202512.2831.v1

19. Miller JD, Kim H, Kjeldsen TR, Packman J, Grebby S, Dearden R. Assessing the impact of urbanization on storm runoff in a peri-urban catchment using historical change in impervious cover. J Hydrol (Amst) 2014;515:59–70. https://doi.org/10.1016/j.jhydrol.2014.04.011.
20. Song X, Sun W, Zhang Y, Song S, Li J, Gao Y. Using hydrological modelling and data-driven approaches to quantify mining activities impacts on centennial streamflow. J Hydrol (Amst) 2020;585. https://doi.org/10.1016/j.jhydrol.2020.124764.
21. Zhang M, Stodolak R, Xia J. The impact of the changes in climate, land use and direct human activity on the discharge in qingshui river basin, china. Water (Switzerland) 2021;13. https://doi.org/10.3390/w13213147.
22. Zimba H, Kawawa B, Chabala A, Phiri W, Selsam P, Meinhardt M, et al. Assessment of trends in inundation extent in the Barotse Floodplain, upper Zambezi River Basin: A remote sensing-based approach. J Hydrol Reg Stud 2018;15:149–70. https://doi.org/10.1016/j.ejrh.2018.01.002.
23. Gao P, Li P, Zhao B, Xu R, Zhao G, Sun W, et al. Use of double mass curves in hydrologic benefit evaluations. Hydrol Process 2017;31:4639–46. https://doi.org/10.1002/hyp.11377.
24. Reis AA dos, Weerts A, Ramos M-H, Wetterhall F, Fernandes W dos S. Hydrological data and modeling to combine and validate precipitation datasets relevant to hydrological applications. J Hydrol Reg Stud 2022;44:101200. https://doi.org/10.1016/j.ejrh.2022.101200.
25. Loots I, Smithers JC, Kjeldsen TR. Quantifying urban land cover imperviousness as input for flood simulation using machine learning: South African case study. Water Science & Technology 2025;91:1141–56. https://doi.org/10.2166/wst.2025.067.
26. Urzică A, Mihu-Pintilie A, Stoleriu CC, Cîmpianu CI, Huţanu E, Pricop CI, et al. Using 2D HEC-RAS modeling and embankment dam break scenario for assessing the flood control capacity of a multireservoir system (Ne Romania). Water (Switzerland) 2021;13. https://doi.org/10.3390/w13010057.
27. Neal JC, Fewtrell TJ, Bates PD, Wright NG. A comparison of three parallelisation methods for 2D flood inundation models. Environmental Modelling & Software 2010;25:398–411. https://doi.org/10.1016/j.envsoft.2009.11.007.
28. Griffiths J, Borne KE, Semadeni-Davies A, Tanner CC. Selection, Planning, and Modelling of Nature-Based Solutions for Flood Mitigation. Water (Basel) 2024;16:2802. https://doi.org/10.3390/w16192802.
29. Long'or Lokidor P, Taka M, Lashford C, Charlesworth S. Nature-based Solutions for sustainable flood management in East Africa. J Flood Risk Manag 2023;17. https://doi.org/10.1111/jfr3.12954.
30. USACE. HEC-RAS User's Manual. 2024.
31. LWSC. Lusaka Water Sanitation and Drainage Project. Lusaka: 2013.
32. Nick A. Groundwater Resources for Lusaka and selected Catchment Areas. Lusaka: 2015.
33. Chomba IC. Sedimentation and its Effects on Selected Small Dams in Lusaka Province, Zambia. Lusaka: 2017.
34. Tena TM, Mudenda F, Nguvulu A, Mwaanga P, Gathenya JM. Analysis of River Tributaries' Streamflow Contribution Using WEAP Model: A Case of the Ngwerere and Kanakatampa Tributaries to the Chongwe River in Zambia. J Water Resour Prot 2021;13:309–23. https://doi.org/10.4236/jwarp.2021.134019.
35. Tena TM, Mwaanga P, Nguvulu A. Hydrological modelling and water resources assessment of Chongwe River Catchment using WEAP model. Water (Switzerland) 2019;11. https://doi.org/10.3390/w11040839.
36. Chabwela H, Chomba C, Chabwela B, Muyumbana N. Vegetation Structure and Condition of the Head Water Palustrine Dambo Eco-System in the Upper Catchment of the Chongwe River, Central Zambia. IAR Journal of Agriculture Research and Life Sciences 2021;2:55–74.
37. MCC. Improving Water, Sanitation, and Drainage in Zambia: Partial Progress on Strengthening Service Delivery and Financial Sustainability. 2020.
38. Tena TM, Mwaanga P, Nguvulu A. Impact of land use/land cover change on hydrological components in Chongwe River Catchment. Sustainability (Switzerland) 2019;11. https://doi.org/10.3390/su11226415.
39. JICA. Basic Design Study Report on New Agricultural Village Development Project in Kanakantapa Area, Lusaka Province in the Republic of Zambia. Lusaka: 1991.
40. Heberger M. Global Watersheds (web application) 2022.

41. Japan Aerospace Exploration Agency. ALOS World 3D 30 meter DEM 2021. https://doi.org/https://doi.org/10.5069/G94M92HB.
42. Ross CW, Prihodko L, Anchang JY, Kumar SS, Ji W, Hanan NP. Global Hydrologic Soil Groups (HYSOGs250m) for Curve Number-Based Runoff Modeling, 2018. https://doi.org/10.3334/ORNLDAAC/1566.
43. Hoppe A. Simulation of flooding and flood mitigation in the town of Söderköping using HEC-RAS An investigation of floods and mitigation measures. 2023.
44. Lima Neto OC, Ribeiro Neto A, Alves FHB, Cirilo JA. Sub-daily hydrological-hydrodynamic simulation in flash flood basins: Una river (Pernambuco/Brazil). Ambiente e Agua - An Interdisciplinary Journal of Applied Science 2020;15:1. https://doi.org/10.4136/ambi-agua.2556.
45. Akiyanova F, Ongdas N, Zinabdin N, Karakulov Y, Nazhbiyev A, Mussagaliyeva Z, et al. Operation of Gate-Controlled Irrigation System Using HEC-RAS 2D for Spring Flood Hazard Reduction. Computation 2023;11. https://doi.org/10.3390/computation11020027.
46. Chow VT. Open Channel Hydraulics. New York: McGraw-Hill; 1959.
47. USDA SCS. Urban hydrology for small watersheds. Washington, DC: 1986.
48. Ficklin DL, Abatzoglou JT, Robeson SM, Dufficy A. The Influence of Climate Model Biases on Projections of Aridity and Drought. J Clim 2016;29:1269–85. https://doi.org/10.1175/JCLI-D-15-0439.1.
49. Sarker S. Separation of Floodplain Flow and Bankfull Discharge: Application of 1D Momentum Equation Solver and MIKE 21C. CivilEng 2023;4:933–48. https://doi.org/10.3390/civileng4030050.
50. Bates PD, Horritt MS, Fewtrell TJ. A simple inertial formulation of the shallow water equations for efficient two-dimensional flood inundation modelling. J Hydrol (Amst) 2010;387:33–45. https://doi.org/10.1016/j.jhydrol.2010.03.027.
51. Borst R. Evaluating the Effect of Nature-Based Solutions on Urban Runoff Using Hydraulic Modelling: A Case Study in Sekondi-Takoradi, Ghana. 2023.
52. Blue Marble Geographics. Global Mapper Pro v26.0 2024.
53. Zeiger SJ, Hubbart JA. Measuring and modeling event-based environmental flows: An assessment of HEC-RAS 2D rain-on-grid simulations. J Environ Manage 2021;285. https://doi.org/10.1016/j.jenvman.2021.112125.
54. Chisola MN, Kuráž M. Patterns and Implications of Hydrologic Regime Change in Chongwe River, Zambia. Journal of Geography and Geology 2016;8:1. https://doi.org/10.5539/jgg.v8n3p1.
55. Tang Z, Chu J, Zhou Z, Zhou T, Yuan K. The Sensitivity Analysis of Parameters in the 1D–2D Coupled Model for Urban Flooding. Applied Sciences 2025;15:2157. https://doi.org/10.3390/app15042157.
56. Morris MD. Factorial Sampling Plans for Preliminary Computational Experiments. Technometrics 1991;33:161–74. https://doi.org/10.1080/00401706.1991.10484804.
57. Timalsina H, Hwang S, Cooke RA, Bhattarai R. Comparative Sensitivity Analysis of Hydrology and Relative Corn Yield under Different Subsurface Drainage Design Using DRAINMOD. Applied Sciences 2023;13:9252. https://doi.org/10.3390/app13169252.
58. Zhang Z, Liao W, Chen H, Mantini D, Ding J-R, Xu Q, et al. Altered functional–structural coupling of large-scale brain networks in idiopathic generalized epilepsy. Brain 2011;134:2912–28. https://doi.org/10.1093/brain/awr223.
59. McColgan P, Blom T, Rees G, Seunarine KK, Gregory S, Johnson E, et al. Stability and sensitivity of structural connectomes: effect of thresholding and filtering and demonstration in neurodegeneration 2018. https://doi.org/10.1101/416826.
60. Afzal MA, Ali S, Nazeer A, Khan MI, Waqas MM, Aslam RA, et al. Flood Inundation Modeling by Integrating HEC–RAS and Satellite Imagery: A Case Study of the Indus River Basin. Water (Basel) 2022;14:2984. https://doi.org/10.3390/w14192984.
61. Moriasi DN, Gitau MW, Pai N, Daggupati P. Hydrologic and water quality models: Performance measures and evaluation criteria. Trans ASABE 2015;58:1763–85. https://doi.org/10.13031/trans.58.10715.
62. Ndhlovu GZ, Woyessa YE. Streamflow Analysis in Data-Scarce Kabompo River Basin, Southern Africa, for the Potential of Small Hydropower Projects under Changing Climate. Hydrology 2022;9. https://doi.org/10.3390/hydrology9080149.

 doi:10.20944/preprints202512.2831.v1

63. Belay H, Melesse AM, Tegegne G, Kassaye SM. Flood Inundation Mapping Using the Google Earth Engine and HEC-RAS Under Land Use/Land Cover and Climate Changes in the Gumara Watershed, Upper Blue Nile Basin, Ethiopia. Remote Sens (Basel) 2025;17:1283. https://doi.org/10.3390/rs17071283.
64. Alipour A, Jafarzadegan K, Moradkhani H. Global sensitivity analysis in hydrodynamic modeling and flood inundation mapping. Environmental Modelling & Software 2022;152:105398. https://doi.org/10.1016/j.envsoft.2022.105398.
65. Bennour A, Jia L, Menenti M, Zheng C, Zeng Y, Barnieh BA, et al. Calibration and Validation of SWAT Model by Using Hydrological Remote Sensing Observables in the Lake Chad Basin. Remote Sens (Basel) 2022;14. https://doi.org/10.3390/rs14061511.
66. YEC. Study Report on National Water Resources Master Plan in the Republic of Zambia. Lusaka, Zambia: 1995.
67. Velísková Y, Dulovičová R, Schügerl R. Impact of vegetation on flow in a lowland stream during the growing season. Biologia (Bratisl) 2017;72:840–6. https://doi.org/10.1515/biolog-2017-0095.
68. Palanisamy B, Chui TFM. Rehabilitation of concrete canals in urban catchments using low impact development techniques. J Hydrol (Amst) 2015;523:309–19. https://doi.org/10.1016/j.jhydrol.2015.01.034.
69. Wright IA, Davies PJ, Findlay SJ, Jonasson OJ. A new type of water pollution: concrete drainage infrastructure and geochemical contamination of urban waters. Mar Freshw Res 2011;62:1355–61. https://doi.org/10.1071/MF10296.
70. Sarker S. A Short Review on Computational Hydraulics in the Context of Water Resources Engineering. Open Journal of Modelling and Simulation 2021;10:1–31. https://doi.org/10.4236/ojmsi.2022.101001.
71. Gruss Ł, Głowski R, Wiatkowski M. Modeling of water flows through a designed dry dam using the HEC-RAS program. ITM Web of Conferences 2018;23:00012. https://doi.org/10.1051/itmconf/20182300012.
72. C. Chomba I, M. Sichingabula H. Sedimentation and Its Effects on Selected Small Dams East of Lusaka, Zambia. Modern Environmental Science and Engineering 2016;1:325–40. https://doi.org/10.15341/mese(2333-2581)/06.01.2015/007.
73. Lempérière F. Dams and Floods. Engineering 2017;3:144–9. https://doi.org/10.1016/J.ENG.2017.01.018.
74. Khoeun R, Sor R, Chann K, Phy SR, Oeurng C, Sok T. The Impacts of Dams on Streamflow in Tributaries to the Lower Mekong Basin. Sustainability 2024;16:6700. https://doi.org/10.3390/su16156700.
75. Olariu P, Cojoc GM, Tirnovan A, Obreja F. The future of reservoirs in the Siret River Basin considering the sediment transport of rivers (Romania) 2014. https://doi.org/10.4316/GEOREVIEW.2014.24.1.169.
76. Peter SJ, De Araújo JC, Araújo NAM, Herrmann HJ. Flood avalanches in a semiarid basin with a dense reservoir network. J Hydrol (Amst) 2014;512:408–20. https://doi.org/10.1016/j.jhydrol.2014.03.001.
77. Nguvulu A, Shane A, Mwale CS, Tena TM, Mwaanga P, Siame J, et al. Surface Water Quality Response to Land Use Land Cover Change in an Urbanizing Catchment: A Case of Upper Chongwe River Catchment, Zambia. Journal of Geographic Information System 2021;13:578–602. https://doi.org/10.4236/jgis.2021.135032.
78. Erhui L, Mu X, Zhao G, Gao P, Sun W. Effects of check dams on runoff and sediment load in a semi-arid river basin of the Yellow River. Stochastic Environmental Research and Risk Assessment 2017;31:1791–803. https://doi.org/10.1007/s00477-016-1333-4.
79. Sang J, Gatheny M, Ndegwa G. Evaluation of reservoirs as flood mitigation measure in Nyando basin, western Kenya using swat 2007;18:231–9.
80. Acheampong JN, Gyamfi C, Arthur E. Impacts of retention basins on downstream flood peak attenuation in the Odaw river basin, Ghana. J Hydrol Reg Stud 2023;47:101364. https://doi.org/10.1016/j.ejrh.2023.101364.